

**Exploring Peptides as Template Scaffolds for Directed Olefin  
Metathesis Oligomerization**

Thesis by

Katherine G. Poulin-Kerstien

In Partial Fulfillment of the Requirements

for the Degree of

Masters of Science

California Institute of Technology

Pasadena, California

2008

© 2008

Katherine G. Poulin-Kerstien

All Rights Reserved

*...for Adam...*

## **Acknowledgments**

First, I would like to thank my family for all their support and love – I couldn't have made it through this long journey without you. I would also like to thank all of the wonderful friends I've made during my time at Caltech, especially the "traveling scrapbook" ladies and my Snatch teammates, for making grad school a more enjoyable place to be all these years. To my labmates from both of the labs I spent time in, thank you for all your help, encouragement and commiseration along the way. Finally, I would like to thank Prof. David Tirrell for taking me into his lab and for always being so supportive of me and my goals.

## Table of Contents

Acknowledgments.....	iv
Table of Contents.....	v
List of Figures and Tables.....	vii
Chapter 1      Introduction: Taking a Cue from Nature.....	1
Chapter 2      A Pseudorotaxane Recognition Motif.....	8
Chapter 3      A Boronate Ester Recognition Motif.....	51

## List of Figures and Tables

<b>Chapter 1</b>		<b>Page</b>
Figure 1.1	PLGA product distribution	2
Figure 1.2	Ruthenium alkylidene metathesis catalysts	4
Figure 1.3	Types of metathesis chemistry	5
 <b>Chapter 2</b>		
Figure 2.1	Structure of a [2]pseudorotaxane	9
Table 2.1	Influence of solvent on [2]pseudorotaxane formation	10
Table 2.2	Series of ammonium-bearing templates studied	11
Figure 2.2	Solid state structure of [3]pseudorotaxane	11
Figure 2.3	Helical peptides	12
Scheme 2.1	Synthesis of <b>P11</b>	14
Figure 2.4	The BArF counterion	16
Figure 2.5	Series of alkane-linked templates, <b>b-Am<sub>A</sub></b>	18
Scheme 2.2	Synthesis of <b>b-Am<sub>B</sub></b>	18
Scheme 2.3	Synthesis of <b>M</b>	19
Scheme 2.4	Synthesis of DB24C8-olefin derivatives	21
Table 2.3	<i>R</i> values for helical peptide templates	22
Figure 2.6	CD spectra of <b>P15</b> at different concentrations	22
Figure 2.7	CD spectra of <b>P11</b> with and without benzyl modification	22
Figure 2.8	CD spectra of <b>P11</b> , <b>P18</b> and <b>P20</b>	23
Figure 2.9	2D <sup>1</sup> H NMR of <b>b-Am<sup>F</sup><sub>P11</sub></b>	24

Figure 2.10	2D NMR couplings	24
Table 2.4	Influence of solvent on <b>M</b> pseudorotaxane formation	26
Table 2.5	Influence of temperature on <b>M</b> pseudorotaxane formation	26
Table 2.6	Influence of equivalents of <b>DB24C8</b> on <b>M</b> pseudorotaxane formation	26
Table 2.7	Influence of Bn <i>p</i> -modification on <b>M</b> pseudorotaxane formation	27
Figure 2.11	ESI-MS of <b>b-Am<sub>P11</sub></b> and <b>DB24C8-CP</b> pseudorotaxane	28
Figure 2.12	<sup>19</sup> F NMR of <b>M-<i>p</i>F</b> and <b>DB24C8-CP</b> pseudorotaxane	30
Figure 2.13	<sup>19</sup> F NMR of <b>b-Am<sub>P11</sub></b> and <b>DB24C8-CP</b> pseudorotaxane	30
Figure 2.14	TOSCY spectra of <b>b-Am<sub>P11</sub></b> without and with <b>DB24C8-5en</b>	32
Figure 2.15	Ruthenium alkylidene metathesis catalysts	33
Table 2.8	Influence of catalysts on template-directed metathesis	33
Table 2.9	Template-directed metathesis with <b>DB24C8-e5en</b>	34
Table 2.10	Influence of benzoquinone on template-directed metathesis	34
Figure 2.16	Binding modes for DB24C8 and benzyl-ammonium ion	35
Figure 2.17	Influence of different sizes of crown-ethers on template-directed metathesis	36
Figure 2.18	Influence of <b>b-Am<sub>P11</sub></b> on <b>DB24C8-CP</b> ROMP	37
Figure 2.19	Influence of <b>b-Am<sub>P11</sub></b> on <b>DB24C8-5en</b> CM	38
Figure 2.20	ESI-MS spectrum of CM reaction of <b>DB24C8-5en</b> with <b>b-Am<sub>P11</sub></b>	39
Table 2.11	Comparison of peptide template-directed CM	40
Table 2.12	Comparison of template-directed ADMET	40
Table 2.13	Comparison of <b>b-Am<sub>A</sub></b> series of templates on ADMET	41
Table 2.14	Influence of template purity on ADMET	42
Table 2.15	Template-directed trimerization	43

### Chapter 3

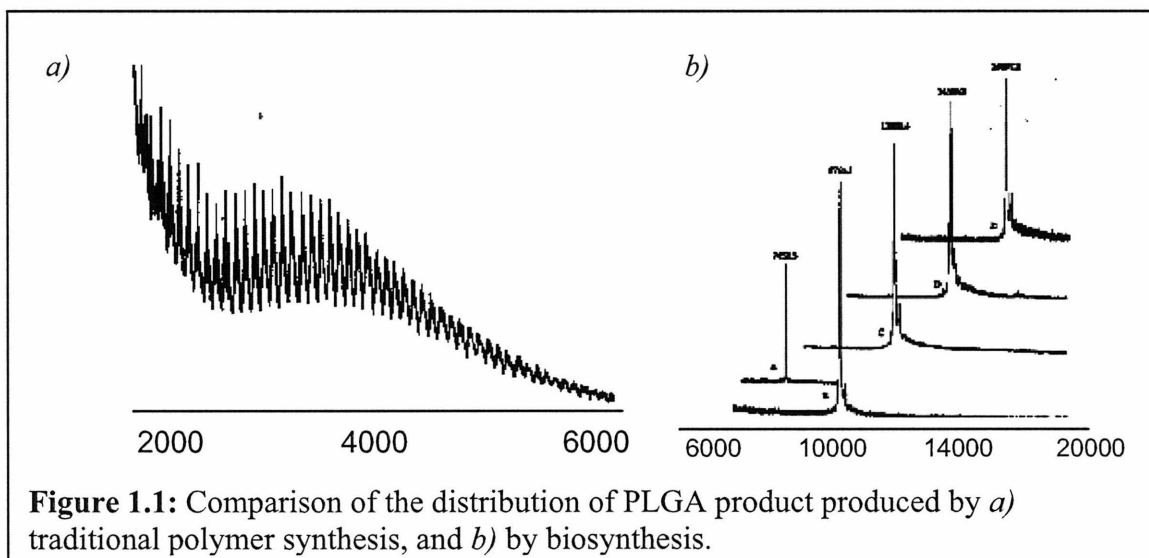
Table 3.1	Boronate ester equilibrium constants	53
Figure 3.1	Boronate ester formation	53
Table 3.2	Series of boronic acid peptide template studied	54
Scheme 3.1	Synthesis of peptide templates	55
Scheme 3.2	Synthesis of diol-olefin monomers	57
Figure 3.2	HPLC analysis of on-resin boronate ester formation and hydrolysis	59
Table 3.3	Influence of <b>b-BA<sub>P3</sub></b> on CM	59
Table 3.4	Influence of <b>b-BA<sub>P3</sub></b> on <b>1,3-diol-diene</b> ADMET	60
Figure 3.3	HPLC analysis of <b>MBHA-b-BA<sub>P3</sub></b> directed ADMET	61
Figure 3.4	HPLC analysis of on-resin tris-templates directed ADMET	62

## **Chapter 1**

*Introduction: Taking a Cue from Nature*

## Background:

Nature employs template-directed synthesis<sup>1-4</sup> by using noncovalent bonds and  $\pi$ - $\pi$  stacking interactions to obtain well-defined biopolymers – DNA, RNA, and proteins – in respect to their precise lengths, specific sequences, and stereochemical purity. This is in contrast to conventional polymerization techniques which give rise to heterogeneous populations of products.<sup>5</sup> For example, the traditional synthesis of poly( $\alpha$ ,L-glutamic acid) (PLGA) via ring-opening polymerization of N-carboxy- $\alpha$ -glutamic acid anhydrides yields products with a broad distribution of molecular weights (**Fig. 1.1a**).<sup>6</sup> On the other hand, harnessing biological machinery to generate PLGA via biosynthetic techniques yields a monodisperse product, with a molecular weight determined at the genetic level (**Fig. 1.1b**).



The versatility of genetically engineered polymer synthesis is limited by Nature's building blocks. DNA and RNA are limited to the five natural nucleotides and proteins are limited to the twenty natural amino acids. Extensive work has been done to expand the available pool of building blocks, including work with modified nucleic acids<sup>7</sup> and

non-canonical amino acids.<sup>8,9</sup> While, peptides and proteins with novel characteristics have been generated by biosynthesis with non-canonical amino acids,<sup>10,11</sup> polymers with drastically different properties might be accessible by means of to a different class of monomers.

### **Examples of Template-Directed Polymerization:**

In an example of highly controlled polymerization, Liu and co-workers successfully used a DNA template to perform synthesis of peptide nucleic acids (PNAs).<sup>12</sup> Employing a four base pair recognition codon, up to five PNA tetramer units were oligomerized in a sequence-dependent fashion via reductive amination chemistry. This experiment demonstrated tight template-controlled polymerization and high product yields. However, the resulting DNA-templated products are themselves DNA-based polymers, retaining characteristics of the template beyond sequence information. In addition to reductive amination, a range of other reactions have been directed by DNA templates in a sequence-specific fashion, including amine acylation, oxazolidine formation, Wittig olefination and the Huisgen cycloaddition.<sup>13</sup> None of these other reactions, however, have been employed for template-directed polymerization.

In recent work, South and Weck demonstrated the template-directed synthesis of an artificial polymer by ruthenium alkylidene mediated olefin metathesis.<sup>14</sup> Ring opening metathesis polymerization (ROMP) of a norbornene-based thymine monomer was directed by a norbornene-polymer template functionalized with diaminopyridine recognition units, yielding a product with a PDI of 1.19. Without the template, ROMP of the thymine monomer yielded a polymer with a PDI of 1.73. While this work

demonstrated a template effect, the template itself was a norbornene polymer generated via ROMP, and so neither it nor the polymer product was monodisperse.

Olefin metathesis,<sup>15, 16</sup> using ruthenium alkylidene catalysts, has been utilized in other templated-directed (non-polymer) syntheses, such as those of mechanically interlocked catenane- and rotaxane-based structures<sup>17-19</sup> and for the dimerization of a hydrogen-bonded oligoamide duplex.<sup>20</sup>

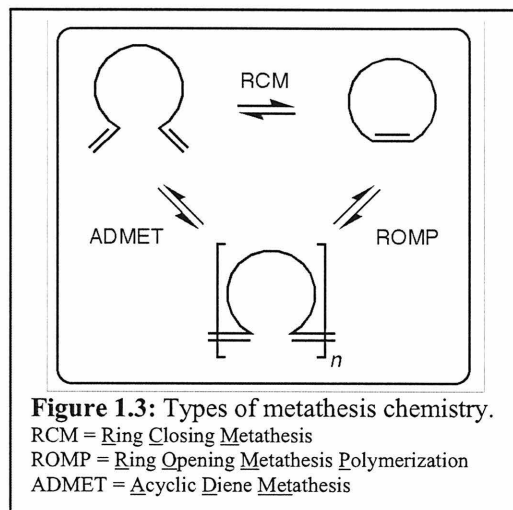
### **Scope of This Work:**

The goal of this research project was to establish a highly controllable method to synthesize non-biologically based heteropolymers. To accomplish this, proteins and peptides were chosen as template scaffolds. By using peptide biopolymers as templates, the cellular machinery of living cells can be utilized to generate the templates. In addition, the well-established techniques of directed evolution<sup>21</sup> can be used to evolve the structure and function of the artificial, templated polymers via manipulation of the templates at the DNA level.

There has also been extensive work done on the designing and controlling the conformational structure of peptides and proteins based upon their primary sequence, making them attractive for templates designed rationally.<sup>22, 23</sup> An additional benefit inherent to a peptide scaffold lies in the versatility of the side chains which have variable functionality and are separate from the linear polymer. The side chains provide a useful means of presenting multiple binding sites without manipulation of the amide backbone.

To synthesize completely artificial heteropolymers with sequences as well-defined as those found in nature, an alternative set of catalysts and molecular recognition motifs had to be identified and developed. Given the previous successes in templated

syntheses and its convenience for polymerizations, olefin metathesis was chosen as the polymerization chemistry for this project. Both ROMP and acyclic diene metathesis (ADMET) – two methods of metathesis polymerization (Fig. 1.3) – are sensitive to the concentration of olefin in solution, and will not proceed below a critical concentration that is



specific for each olefin. For example, the critical concentration at room temperature for cyclopentene is 0.9M, while for cycloheptene it is 0.75M. Thus, if a templated reaction is run below the critical concentration, only monomer coordinated to the template will achieve a local concentration above the critical value. In this way, selective template-directed polymerization will be achieved.

To transfer information from the template to the artificial daughter polymer, selective interactions between the template and its binding partners (i.e., the metathesis monomers) must be designed. This recognition may be based on interactions such as hydrogen bonding, aromatic stacking, electrostatics, or metal-ligand interactions. Utilization of sets of recognition motifs that are orthogonal interactions to one another will enable the generation of ordered heteropolymers, with properties not available via simple homopolymers or random heteropolymers.

Particularly relevant to establishing a template-directed polymerization system is the ability to use thermodynamic control to direct the formation of a well-defined molecular compound during a reaction which, if it were performed under kinetic control

would afford a myriad of products. Thermodynamic control is critical to supramolecular<sup>24</sup> and dynamic covalent chemistry (DCC),<sup>25-27</sup> both of which rely upon reversible non-covalent and covalent bond making and breaking processes as part of key proof-reading and error checking mechanisms. Thus, the success of a thermodynamically controlled protocol depends at the outset on the formation of complexes that are extremely stable prior to polymerization. This criterion must be taken into account when designing a recognition motif.

In this research program, two recognition motifs are investigated: the [2]pseudorotaxane formed between secondary dialkylammonium ions and crown-ethers (Chapter 2), and the boronate ester formed between diols and boronic acids (Chapter 3).

## References

1. Cantrill, S. J.; Pease, A. R.; Stoddart, J. F., *J. Chem. Soc., Dalton Trans.*, **2000**, 3715-3734.
2. Hoss, R.; Vogtle, F., *Angew. Chem. Int. Ed.*, **1994**, *33*, 375-384.
3. Anderson, S.; Anderson, H. L.; Sanders, J. K. M., *Acc. Chem. Res.*, **1993**, *26*, 469-475.
4. Busch, D. H.; Stephenson, N. A., *Coord. Chem. Rev.*, **1990**, *100*, 119-154.
5. Krejchi, M. T.; Atkins, E. D. T.; Waddon, A. J.; Fournier, M. J.; Mason, T. L.; Tirrell, D. A., *Science*, **1994**, *265*, 1427-1432.
6. Zhang, G. H.; Fournier, M. J.; Mason, T. L.; Tirrell, D. A., *Macromolecules*, **1992**, *25*, 3601-3603.
7. Cobb, A. J. A., *Org. Biomol. Chem.*, **2007**, *5*, 3260-3275.
8. Dougherty, M. J.; Kothakota, S.; Mason, T. L.; Tirrell, D. A.; Fournier, M. J., *Macromolecules*, **1993**, *26*, 1779-1781.
9. Connor, R. E.; Tirrell, D. A., *Polymer Rev.*, **2007**, *47*, 9-28.
10. Yoo, T. H.; Link, A. J.; Tirrell, D. A., *Proc. Nat. Acad. Sci U.S.A.*, **2007**, *104*, 13887-13890.
11. Montclare, J. K.; Tirrell, D. A., *Angew. Chem. Int. Ed.*, **2006**, *45*, 4518-4521.
12. Rosenbaum, D. M.; Liu, D. R., *J. Am. Chem. Soc.*, **2003**, *125*, 13924-13925.
13. Calderone, C. T.; Liu, D. R., *Curr. Opin. Chem. Biol.*, **2004**, *8*, 645-653.
14. South, C. R.; Weck, M., *Macromolecules*, **2007**, *40*, 1386-1394.
15. Grubbs, R. H., Ed., *Handbook of Metathesis*. Wiley-VCH: Weinheim, 2003.
16. Trnka, T. M.; Grubbs, R. H., *Acc. Chem. Re.*, **2001**, *34*, 18-29.
17. Badjic, J. D.; Nelson, A.; Cantrill, S. J.; Turnbull, W. B.; Stoddart, J. F., *Acc. Chem. Res.*, **2005**, *38*, 723-732.
18. Guidry, E. N.; Cantrill, S. J.; Stoddart, J. F.; Grubbs, R. H., *Org. Lett.*, **2005**, *7*, 2129-2132.
19. Kilbinger, A. F. M.; Cantrill, S. J.; Waltman, A. W.; Day, M. W.; Grubbs, R. H., *Angew. Chem. Int. Ed.*, **2003**, *42*, 3281-3285.
20. Yang, X. W.; Gong, B., *Angew. Chem. Int. Ed.*, **2005**, *44*, 1352-1356.
21. Xu, H. F.; Zhang, X. E.; Zhang, Y. M.; Cass, A. E. G., *Prog. Biochem. Biophys.*, **2002**, *29*, 518-522.
22. Toniolo, C.; Crisma, M.; Formaggio, F.; Peggion, C.; Broxterman, Q.; Kaptein, B., *J. Inclusion Phenom. Macrocyc. Chem.*, **2005**, *51*, 121-136.
23. Bolin, K. A.; Millhauser, G. L., *Acc. Chem. Res.*, **1999**, *32*, 1027-1033.
24. Lehn, J. M., *Supramo. Chem.*, Wiley-VCH: Weinheim, 1996.
25. Fuchs, B.; Nelson, A.; Star, A.; Stoddart, J. F.; Vidal, S. B., *Angew. Chem. Int. Ed.*, **2003**, *42*, 4220-4224.
26. Rowan, S. J.; Cantrill, S. J.; Cousins, G. R. L.; Sanders, J. K. M.; Stoddart, J. F., *Angew. Chem. Int. Ed.*, **2002**, *41*, 898-952.
27. Lehn, J. M., *Chem. Eur. J.*, **1999**, *5*, 2455-2463.

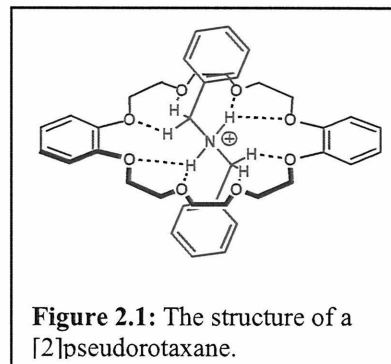
## **Chapter 2**

### ***A Pseudorotaxane Recognition Motif***

## I. Introduction

### The Pseudorotaxane Recognition Motif:

A pseudorotaxane was investigated as a recognition motif in the development of template-directed metathesis polymerization system. A pseudorotaxane is composed of a secondary ammonium ion threaded through an appropriately sized crown-ether molecule stabilized by  $[N^+ - H \cdots O]$  hydrogen bonds and  $[C - H \cdots O]$  interactions (**Fig. 2.1**).<sup>1</sup> This motif is useful in a templating system because it is reversible – allowing easy removal of the daughter template – and its strength is tunable by changes in solvent, temperature or pH. In addition, the secondary ammonium center can be directly generated on a peptide template by the alkylation and protonation of a natural lysine residue.



A rotaxane – derived from the Latin *rota* meaning wheel and *axis* meaning axle – is composed of a macrocyclic compound encircling a rod with two bulky stopper groups at each end. A compound with that composition minus the stoppers is termed a pseudorotaxane and exists in equilibrium between threaded and separated components. The identity of the alkyl groups attached to the ammonium center influences the strength of the pseudorotaxane association.<sup>2</sup> The association constant in deuterated acetonitrile of a [2]pseudorotaxane composed of dibenzo[24]-crown-8 (DB24C8) with dibenzyl ammonium ( $K_a$  of  $420 \text{ L mol}^{-1}$ ) is about five times higher than that of a [2]pseudorotaxane containing dibutyl ammonium ( $K_a$  of  $70 \text{ L mol}^{-1}$ ). This observed difference has been attributed to the increased acidity of the benzylic methylene protons,

which enhances the pseudorotaxane hydrogen-bonding interactions, and to the decreased flexibility of the dibenzyl ammonium moiety, which gives it better preorganization and therefore enhanced binding.

The association constant for pseudorotaxanes is also influenced by solvent. The Gutmann donor number<sup>2</sup> – a semiquantitative measure of the ability of a solvent to participate in non-covalent bonding – varies inversely with the strength of the association in each solvent (**Table 2.1**).<sup>3</sup> For example, the association constant for the [2]pseudorotaxane formed between a dibenzyl ammonium ion and DB24C8 is highest in the solvent with the lowest Gutmann donor number, chloroform, and is zero in the solvent with the highest donor number, DMSO. Notably, in chloroform, the most effective solvent for promoting hydrogen-bonding complex formation, the association constants for the [2]pseudorotaxanes containing dibutyl and dibenzyl ammonium ions are both in the 10<sup>4</sup> range.

Solvent	Gutmann donor no.	K <sub>a</sub> (L mol <sup>-1</sup> )
d <sub>6</sub> -DMSO	29.8	0
d <sub>6</sub> -acetone	17.0	360
CD <sub>3</sub> CN	14.1	420
CDCl <sub>3</sub>	4.0	27000

**Table 2.1:** The effect of solvent on the association constant for a complex of DB24C8 and dibenzyl ammonium ion. (Adapted from Ashton, P.R., *et. al. Chem, Eur. J.*, **1996**, 2(6), 709-728)

### The Templates:

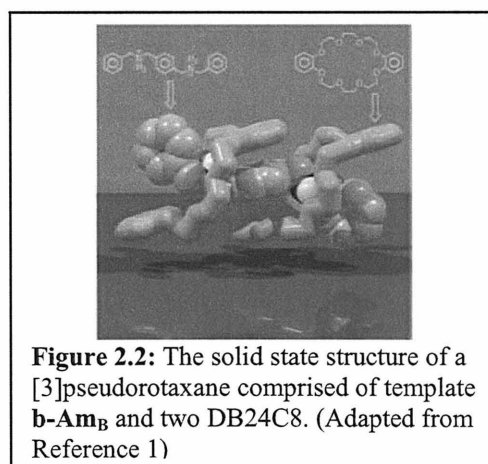
In the investigation of the pseudorotaxane as a recognition motif for the template-directed metathesis system, a number of different templates were evaluated (**Table 2.2**). Within this report, templates with two binding sites, also known as bis-ammonium templates, are denoted as **b-Am**, while the tris-ammonium templates, with three binding

sites, are denoted as **t-Am**. The subscript refers to the style of template.

**Table 2.2:** The series of templates studied bearing ammonium ion recognition sites for DB24C8 binding.

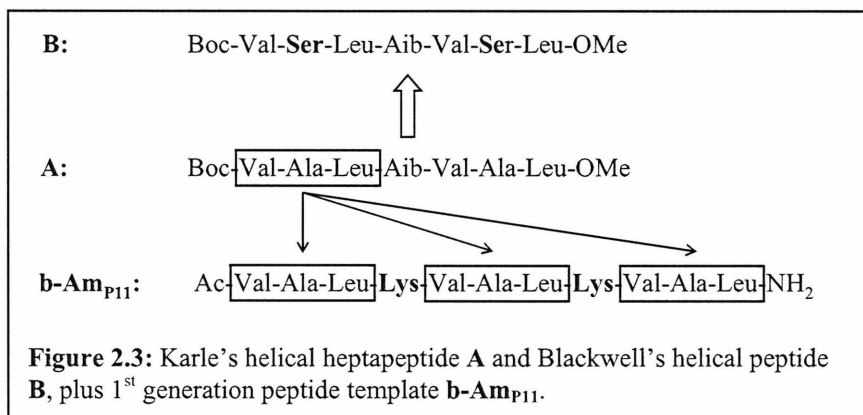
Type of Template	Chemical Formula	ID
Peptide, 11-mer	Ac-VALK <sup>+</sup> (Bn)VALK <sup>+</sup> (Bn)VAL-NH <sub>2</sub>	b-Am <sub>P11</sub>
Peptide, 15-mer	Ac-VALK <sup>+</sup> (Bn)VALK <sup>+</sup> (Bn)VALK <sup>+</sup> (Bn)VAL-NH <sub>2</sub>	t-Am <sub>P15</sub>
Peptide, 20-mer	Ac-VALVALK <sup>+</sup> (Bn)VALVALK <sup>+</sup> (Bn)VALVAL-NH <sub>2</sub>	b-Am <sub>P20</sub>
Peptide, 18-mer	Ac-LALLALLK <sup>+</sup> (Bn)LALAK <sup>+</sup> (Bn)LALLAL-NH <sub>2</sub>	b-Am <sub>P18</sub>
Peptide, 3-mer	Ac-K <sup>+</sup> (Bn)AK <sup>+</sup> (Bn)-NH <sub>2</sub>	b-Am <sub>P3</sub>
Peptide, 5-mer	Ac-K <sup>+</sup> (Bn)AK <sup>+</sup> (Bn)AK <sup>+</sup> (Bn)-NH <sub>2</sub>	t-Am <sub>P5</sub>
Alkane, butane-linked	Bn-(N <sup>+</sup> H <sub>2</sub> )-(CH <sub>2</sub> ) <sub>4</sub> -(N <sup>+</sup> H <sub>2</sub> )-Bn	b-Am <sub>A4</sub>
Alkane, hexane-linked	Bn-(N <sup>+</sup> H <sub>2</sub> )-(CH <sub>2</sub> ) <sub>6</sub> -(N <sup>+</sup> H <sub>2</sub> )-Bn	b-Am <sub>A6</sub>
Alkane, octane-linked	Bn-(N <sup>+</sup> H <sub>2</sub> )-(CH <sub>2</sub> ) <sub>8</sub> -(N <sup>+</sup> H <sub>2</sub> )-Bn	b-Am <sub>A8</sub>
Alkane, decane-linked	Bn-(N <sup>+</sup> H <sub>2</sub> )-(CH <sub>2</sub> ) <sub>10</sub> -(N <sup>+</sup> H <sub>2</sub> )-Bn	b-Am <sub>A10</sub>
Alkane, dodecane-linked	Bn-(N <sup>+</sup> H <sub>2</sub> )-(CH <sub>2</sub> ) <sub>12</sub> -(N <sup>+</sup> H <sub>2</sub> )-Bn	b-Am <sub>A12</sub>
Linear, benzyl-linked	Bn-(N <sup>+</sup> H <sub>2</sub> )-CH <sub>2</sub> -Ph-CH <sub>2</sub> -(N <sup>+</sup> H <sub>2</sub> )-Bn	b-Am <sub>B</sub>
Mono-ammonium, model	TBDPSO-(CH <sub>2</sub> ) <sub>4</sub> -N <sup>+</sup> H <sub>2</sub> -Bn	M

Four different iterations of peptide templates were tested, the designs of which are described in more detail below. In addition, two different types of linear templates were used as standards against which the peptides were compared. Template **b-Am<sub>B</sub>** was known from previous macromolecular studies to bind two DB24C8 molecules (**Fig. 2.2**).<sup>1</sup> The series of alkane-linked linear bis-templates, **b-Am<sub>A</sub>**, were designed to study the influences of template flexibility and binding site spacing on template-directed metathesis.



## Design of 1<sup>st</sup> Generation Peptide Templates:

A helical structure was selected for the first peptide templates because it can be formed by short peptides and is highly ordered, allowing for controlled presentation of the crown-ether binding sites. Also, helices are favored by aprotic, non-polar solvents such as those suitable for metathesis and pseudorotaxane formation.



The design of the 1<sup>st</sup> generation templates, **b-Am<sub>P11</sub>** and **t-Am<sub>P15</sub>**, was based on the Val-Ala-Leu repeat of the helical, hydrophobic heptapeptide (**A** in **Fig. 2.3**) of Karle *et. al.*<sup>4</sup>. Peptide **A** had also inspired the heptapeptide (**B**), developed by Blackwell *et. al.*,<sup>5</sup> which was shown to adopt an  $\alpha$ -helical conformation in the solid state and a  $3_{10}$ -helical conformation in chloroform. In addition, peptide **B** was used in ring closing metathesis reactions, after modification of the serine residues with allyl ethers. For the 1<sup>st</sup> generation peptides, the valine-alanine-leucine repeat was utilized to promote helix formation. The  $\alpha$ -aminoisobutyric acid residue (Aib) is known to stabilize helical conformations. However, Aib residues were not incorporated into the peptide templates because their incorporation by standard biosynthetic expression techniques is not possible. Instead, to adapt the previous sequences to the requirements of a template for pseudorotaxane complex formation, ammonium binding sites were installed via lysine amino acids at

residues  $i$  and  $i+4$  within the peptide sequence. This spacing positions two residues on the same side of the helix, approximately one turn away from each other.

### **Design of 2<sup>nd</sup> Generation Peptide Templates:**

Two longer peptide templates were designed to provide space between the binding sites and greater helical stability compared to the 1<sup>st</sup> generation peptides. The template **b-Am<sub>P20</sub>** used the same valine-alanine-leucine repeat as **b-Am<sub>P11</sub>** and **t-Am<sub>P15</sub>**. However, this peptide is extended by an additional three V-A-L repeats, one on each end and one in between the lysine residues. By increasing the peptide length by nine amino acids, the helical conformation of this template was hypothesized to have increased stability compared to the **b-Am<sub>P11</sub>**. In addition, the spacing between the ammonium centers is  $i$  and  $i+7$ , which places the sites on the same side of an  $\alpha$ -helix two helical turns apart. This makes the binding sites approximately twice the distance of those with  $i$  and  $i+4$  spacing in **b-Am<sub>P11</sub>** (approximately 11.4 angstroms vs. 5.7 angstroms).

The other 2<sup>nd</sup> generation peptide was designed with the sequence Ac-LALLALKLALALKLALLAL-NH<sub>2</sub> to incorporate the more helix-inducing leucine amino acid in the place of valine residues from the V-A-L sequence. The spacing between the lysine residue binding sites was  $i$  and  $i+6$ , which positions the sites on the same side of a  $3_{10}$ -helix (approximately 12.6 angstroms apart). Unfortunately, a synthesis error yielded a peptide missing one leucine residue between the lysine binding sites and gave the template **b-Am<sub>P18</sub>** instead. This template has an  $i$  and  $i+5$  spacing between the lysine residues, which in both  $\alpha$ - and  $3_{10}$ -helices places the binding sites on opposite sides of the helix.

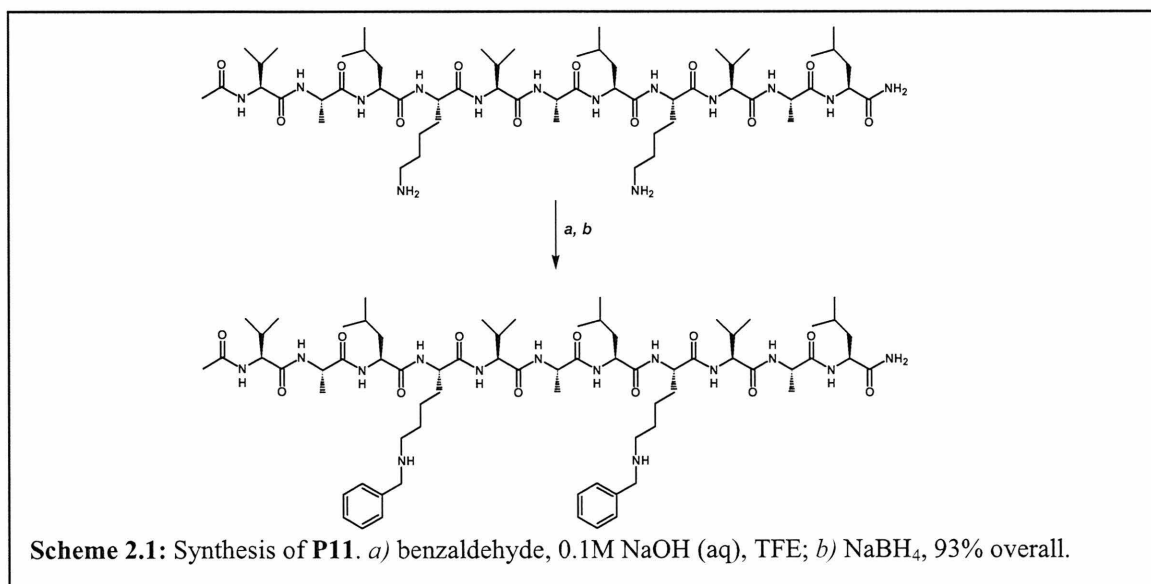
## Design of 3<sup>rd</sup> Generation Templates:

The last set of peptide templates, **b-Am<sub>P3</sub>** and **t-Am<sub>P5</sub>**, was designed to simplify the template motif. These short peptides, consisting of alternating lysine residues – the crown-ether binding sites – and alanine-residue spacers, were not intended to adopt an ordered structure. Rather, they were designed to provide a simple scaffold to hold bound crown-ether molecules in close proximity.

## II. Results and Discussion

### Synthesis of **b-Am<sub>P11</sub>** and **t-Am<sub>P15</sub>** Templates:

The peptide starting materials for the 1<sup>st</sup> generation peptide templates, **b-Am<sub>P11</sub>** and **t-Am<sub>P15</sub>**, were synthesized by the Biopolymer Synthesis and Analysis Facility at the California Institute of Technology and were used without further purification. To provide binding sites for the DB24C8 monomers, the free lysine residues were modified with benzyl groups and protonated.



Complete mono-benzyl protection of both lysine residues of the peptide starting material for **P11** was achieved under reductive amination conditions (**Scheme 2.1**). First, a Schiff base was formed between the free amines of the lysine residues and benzaldehyde in basic solution. Then the intermediate Schiff base was reduced with sodium borohydride to give the desired benzyl-amine product. For **P11**, it was necessary to add benzaldehyde batchwise in three rounds and to employ a time delay before addition of the reducing agent to achieve complete benzyl modification. Attempts to purify **P11** by normal phase column chromatography and prep TLC caused degradation of the peptide, so the crude product was used without further purification.

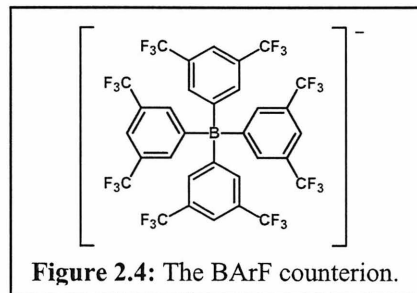
The secondary nitrogen centers of the benzyl-lysine residues of **P11** had to be converted to cationic ammonium centers to enable pseudorotaxane formation. The crown-ether ammonium interaction is maximized by using ammonium salts for which there is weak ion pairing between the ammonium ion and the counterion.<sup>2</sup> The standard counterion used to meet this criterion is hexafluorophosphate ( $\text{PF}_6^-$ ). As an additional benefit, the  $\text{PF}_6^-$  anion often enhances the organic solubility of ammonium salts.

To protonate the peptide and generate the  $\text{PF}_6^-$ -salt, **P11** was mixed with  $\text{HPF}_6$ . ESI-MS confirmed that the reaction had quantitatively generated the doubly charged peptide  $\text{P11}^{2+}$ . However, the  $\text{PF}_6^-$ -salt of  $\text{P11}^{2+}$  was not soluble in chloroform or dichloromethane without the addition of TFE. TFE reduces the pseudorotaxane interaction, making it unsuitable for this templating system.

The large, hydrophobic counterion BArF (**Fig. 2.4**) was tested for its ability to improve the solubility of the protonated peptide. To generate the BArF-salt of **P11** a HBarF-complex was generated in situ.<sup>6</sup> This complex,  $[\text{H}(\text{Et}_2\text{O})_2]^+[\text{BArF}]^-$ , was

successfully made by mixing an anhydrous solution of HCl in ether with NaBArF at reduced temperature.

The NaCl by-product was removed by filtration and the ether was removed to yield the complex as a white solid. At reduced temperature, the  $[\text{H}(\text{Et}_2\text{O})_2]^+[\text{BArF}]^-$



solid was redissolved in anhydrous ether and was added to a solution of **P11**. The reaction yielded a product with an accurate 1:2 peptide to BArF ion ratio. Generation of **P11**<sup>2+</sup> was confirmed by ESI-MS, which showed both the doubly charged peptide and the BArF<sup>-</sup> counterion. The product, **b-Am<sub>P11</sub>**, was found to be readily soluble in chloroform and dichloromethane, and was used for complexation and metathesis studies.

The tris-ammonium template, **t-Am<sub>P15</sub>**, was synthesized using the same procedures described for **b-Am<sub>P11</sub>**.

#### Synthesis of **b-Am<sub>P18</sub>** and **b-Am<sub>P20</sub>** Templates:

The peptide starting materials for two longer templates were ordered from the GenScript Cooperation in crude form. The peptide for **P18** was synthesized by mistake instead of the desired sequence of **P19**, but given the extended time of synthesizing the peptides, complexation and metathesis studies were done with **P18** before it was decided whether or not to order the correct peptide for **P19**.

Using the same reductive amination procedure as with **P11**, the lysine residues of **P20** and **P18** were benzyl protected. Because of the difficulties experienced while trying to purify **P11**, purification of benzylated products **P20** and **P18** was not attempted.

Protonation and coordination with the BArF anions was accomplished using the HBArF-complex.

### Synthesis of **b-Am<sub>P3</sub>** and **t-Am<sub>P5</sub>** Template:

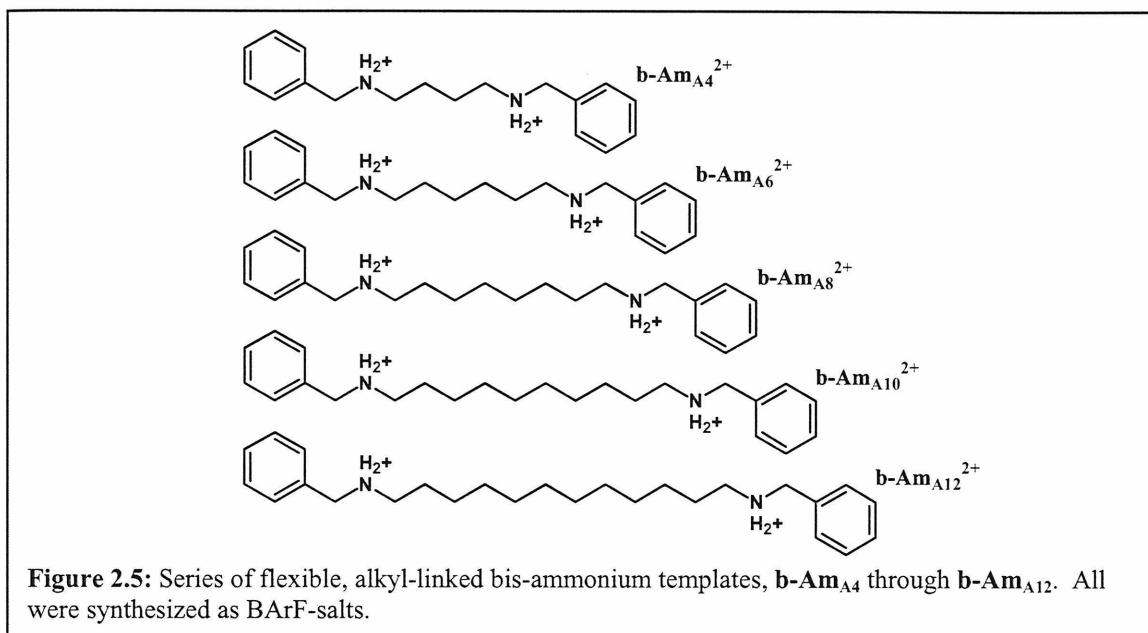
The peptide for template **b-Am<sub>P3</sub>** was synthesized and purified to 97% purity by GenScript. After the initial experiments, further batches of **b-Am<sub>P3</sub>** and **t-Am<sub>P5</sub>** were synthesized by standard Fmoc solid phase peptide synthesis methods. For these templates, a slightly modified procedure was used for the benzyl protected of the lysine residues via reductive amination. As before, a Schiff base was formed between the amine residues of **P3** or **P5** and benzaldehyde. However, in this procedure the imine material was isolated and dried to remove excess benzaldehyde. The reaction material was re-dissolved and the imine was reduced. The crude reaction was purified by reverse phase HPLC and pure **P3<sup>2+</sup>** and **P5<sup>2+</sup>** were isolated as TFA-salts.

To enhance the solubility of **P3<sup>2+</sup>** and **P5<sup>2+</sup>** in organic solvents, the TFA counterions were changed to BArF ions. To accomplish this, pure peptide was dissolved in a minimal amount of water, and dichloromethane was added to make a biphasic solution. NaBArF was added (2 equiv. for **P3<sup>2+</sup>**, and 3 equiv. for and **P5<sup>2+</sup>**), and after vigorous stirring, the templates were isolated from the organic layer. <sup>1</sup>H NMR verified the correct 1:2 or 1:3 peptide to ion ratio.

### Synthesis of **b-Am<sub>A</sub>** Series of Templates:

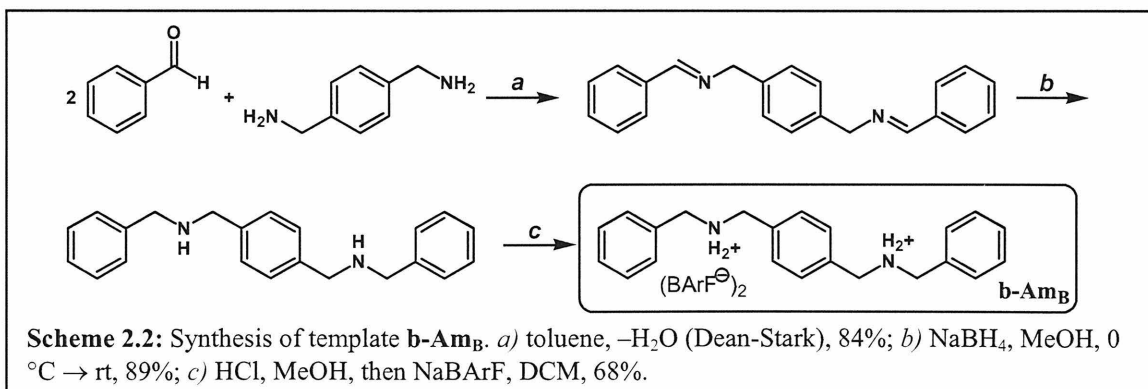
To study both the influence on template-promoted metathesis of template rigidity and the influence of spacing between the crown-ether binding sites, a series of alkane-linked bisammonium templates of varying lengths was synthesized (**Fig. 2.5**). Briefly, each commercially available alkane diamine was benzyl protected under standard reductive amination conditions and purified by column chromatography. The purified dibenzyl-amine products were protonated with HCl, and the resulting HCl-salt

precipitates were isolated. Then, the chloride counterions were replaced by BArF counterions in a biphasic solution of dichloromethane and water.



### Synthesis of **b-Am<sub>B</sub>**:<sup>7</sup>

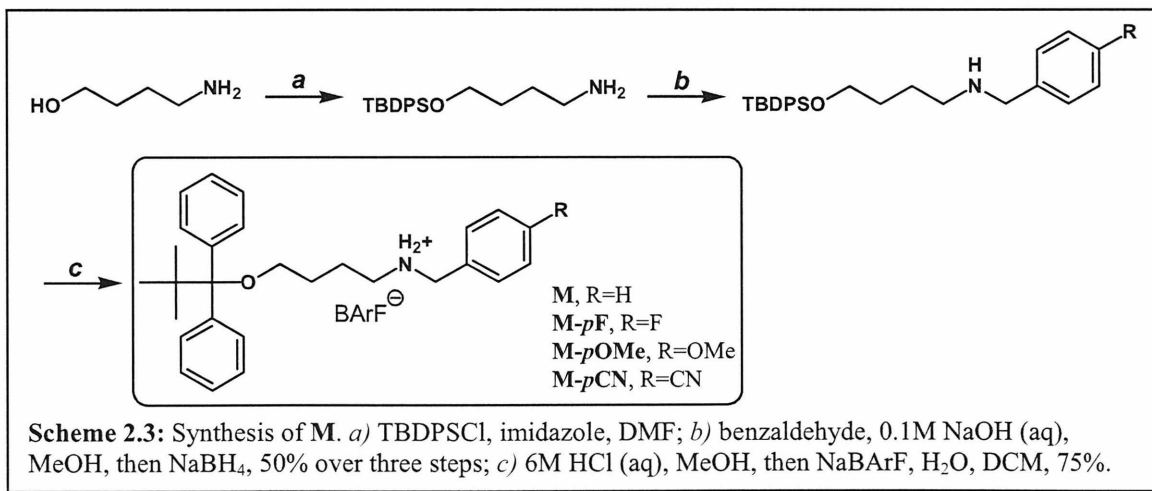
A rigid, linear bis-ammonium template inspired by a previously studied [3]pseudorotaxane system<sup>2</sup> was synthesized as shown in **Scheme 2.2**. Under Dean Stark conditions, *p*-xylylenediamine and two equivalents of benzaldehyde were reacted to give the diimine intermediate. Reduction with sodium borohydride, followed by protonation of the amines with hydrochloric acid and counterion exchange with NaBArF yielded the organic soluble bis-ammonium template.



## Model Synthesis:

A model compound (**M**) was designed to simplify the evaluation of the pseudorotaxane interaction within the peptide template system. To suit this purpose **M** was designed to mimic a benzyl-modified lysine residue. **M** is composed of two parts, a benzyl-protected butylamine moiety that mimics the benzyl-lysine binding site and a bulky t-butyl diphenyl silyl (TBDPS)-protected alcohol that stands in for the peptide chain.

To synthesize **M** (Scheme 2.3), 4-aminobutanol was TBDPS-protected using TBDPS-Cl and imidazole in DMF. The TBDPS group is not only bulky enough to block DB24C8 dissociation,<sup>8</sup> but is also stable to both the basic conditions of the benzylation reaction ( $\text{pH} < 10$ ) and the acidic conditions of the protonation step ( $\text{pH} > 2$ ). Following silyl protection of the alcohol, the amine functionality was mono-benzyl protected using reductive amination conditions. The purified material was protonated in a solution of methanol acidified to  $\text{pH} 2.5$  with an aqueous solution of 6M hydrochloric acid. Finally, NaBArF was used to replace the chloride counterion in a biphasic solution of water and chloroform. Protonated **M** was isolated from the organic layer.

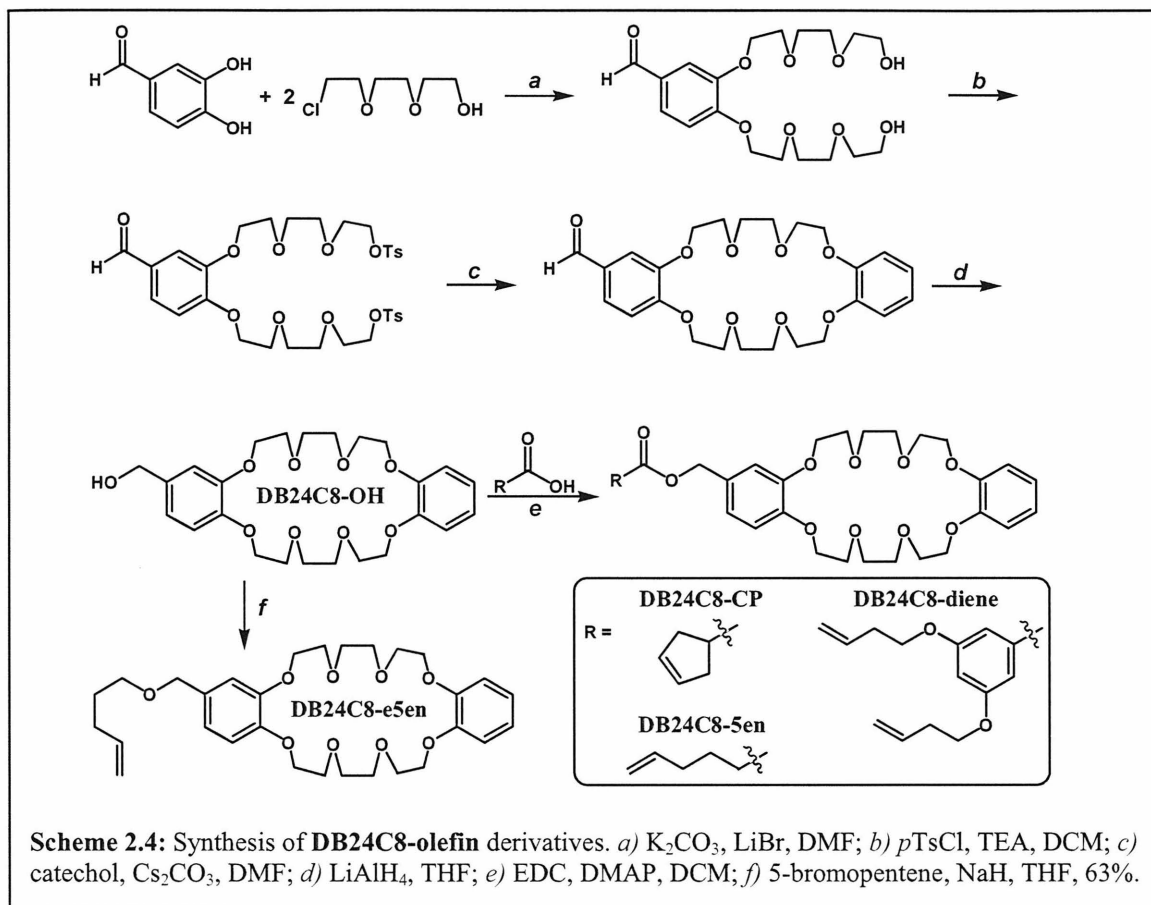


Modification of the benzyl group at the *para*-position with an electron-withdrawing functionality was hypothesized to promote ammonium interaction with the crown-ether. To test this, **M** compounds with *para*-modified benzyl functionalities were synthesized using the same procedure as for **M** but with modified benzaldehyde reagents in the reductive amination step. The functionalities of the three *para*-modified **M** compounds synthesized – fluorine, methoxy and cyano – were chosen because of their range of electron-withdrawing character and because the necessary benzaldehyde reagents were commercially available.

#### **DB24C8-Monomer Syntheses:**

An alcohol modified crown-ether derivative (**DB24C8-OH**) was synthesized and further functionalized with various olefinic moieties (**Scheme 2.4**). To synthesize **DB24C8-OH**, one equivalent of dihydroxybenzaldehyde was treated with two equivalents of 2-[2-(2-chloroethoxy)ethoxy]ethanol. The hydroxyl groups of the diol were tosyl-protected. Macrocyclization with catechol, followed by reduction of the aldehyde with lithium aluminum hydride yielded **DB24C8-OH**. Subsequent EDC coupling to various olefinic acids yielded the ester-functionalized derivatives, **DB24C8-CP**, **-5en** and **-diene**. Alternatively, coupling of **DB24C8-OH** to 5-bromopentene yielded the ether-functionalized derivative **DB24C8-e5en**.

The diene functionality of **DB24C8-diene** was designed to minimize intramolecular metathesis reactions between the two olefins.<sup>9</sup> The acid-containing compound used to couple to **DB24C8-OH** was synthesized by alkylation of methyl 3,5-dihydroxybenzoate with 1-bromobutene and potassium carbonate. Saponification using potassium hydroxide in water and ethanol yielded the acid compound.



### Peptide Conformations:

CD spectra of **P11**, **P15**, **P18** and **P20** were taken in trifluoroethanol. TFE is known to induce peptide conformations similar to those induced by chloroform and dichloromethane,<sup>5</sup> which are the ideal solvents for metathesis chemistry and pseudorotaxane association, but are not suitable for CD spectroscopy. Wavelength scans from 260 nm to 190 nm were taken at room temperature for each peptide.

The CD spectra indicate that all the peptides adopt right-handed  $3_{10}$ -helical conformations in TFE. The  $3_{10}$ -helix is more tightly wound than an  $\alpha$ -helix and has 1 $\leftarrow$ 4 main chain hydrogen bonding, as compared to the 1 $\leftarrow$ 5 pattern found in an  $\alpha$ -helix.<sup>10</sup> CD spectra of helical peptides are distinguished by two minima: one at 206 nm, which

Peptide	$R$
<b>P11</b>	0.55
<b>P18</b>	0.64
<b>P20</b>	0.66

**Table 2.3:**  $R$  values for peptide templates.

arises from a  $\pi$ - $\pi^*$  transition, and another at 222 nm, which arises from a  $n$ - $\pi^*$  transition. A  $3_{10}$ -helix gives rise to a weaker  $n$ - $\pi^*$  transition. This is reflected in a ratio  $R$  – defined

as  $[\Theta]_{222}/[\Theta]_{206}$  – of approximately 0.4. For an  $\alpha$ -helix, the two transitions are approximately equal, giving an  $R$  close to 1.0. The  $R$  values for all the peptides are between 0.55 and 0.66, indicating that the structures of the peptides are mainly  $3_{10}$ -helix, with varying amounts of contaminating  $\alpha$ -helix conformation (**Table 2.3**). The helical structure of **P11** has the most  $3_{10}$ -helical character, while **P20** has the least.

The CD spectra of the bis-ammonium peptides were all found to be independent of concentration, which demonstrates that their structures are monomeric. However, the CD spectra of the tris-ammonium **P15** showed concentration dependence, indicating the formation of higher order aggregates in those samples (**Fig. 2.6**).<sup>11</sup>

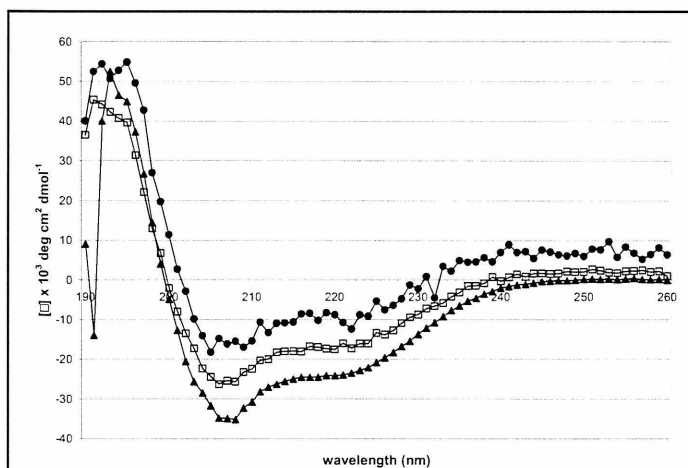


**Figure 2.6:** Concentration dependent CD spectra of **P15**; ● 10 $\mu$ M, □ 30 $\mu$ M, ▲ 100 $\mu$ M.

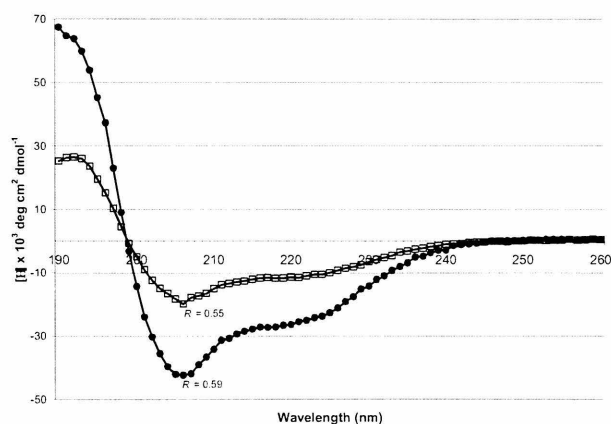
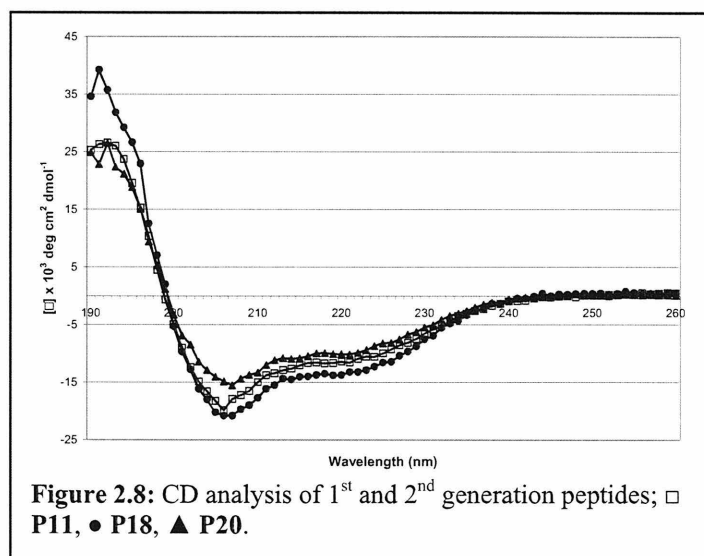


**Figure 2.7:** Influence of Bn-modification on **P11** helicity; ● peptide starting material for **P11** with free lysines, □ **P11**.

As judged by CD analysis in TFE, upon benzyl modification of P11 the strength of the helix formed by the peptide decreases. The starting material peptide for P11 has more than twice the helical character of the benzyl-modified template P11 (Fig. 2.7). It is unclear why benzyl-protection of the lysine residues decreases the peptide helicity.

The CD spectra of P11, P18 and P20 all have similar minima at 206 nm and 220 nm (Fig. 2.8). Thus, in opposition to the design principle of the P18 and P20 templates, the longer sequences did not endow them with increased helical character compared to P11.



A melting curve of P18 from 25 °C to 72 °C showed a gradual decrease in helicity, but no distinct phase transition. A similar result was seen with P11. This type of melting behavior is indicative of a peptide existing in multiple conformations.

#### NMR Analysis of the Conformation of b-Am<sub>P11</sub>:

A series of 2D NMR spectra – tntocsy, and tnoesy – were taken to explore the conformation of one of the peptide templates, fluorinated b-Am<sub>P11</sub> (dubbed b-Am<sup>F</sup><sub>P11</sub>), in deuterated dichloromethane. Tntocsy and tnoesy data were acquired for three different samples of b-Am<sup>F</sup><sub>P11</sub>. All eleven spin systems were identifiable in all three tntocsy spectra, although each sample gave different results (Fig. 2.9). Extensive heating and sonication of one of the samples changed its spectrum slightly, but not enough so that it matched either of the other two samples. This disparity indicates that each batch of b-

$\text{Am}^{\text{F}}_{\text{P11}}$  folded differently, even though the preparation procedures were identical.

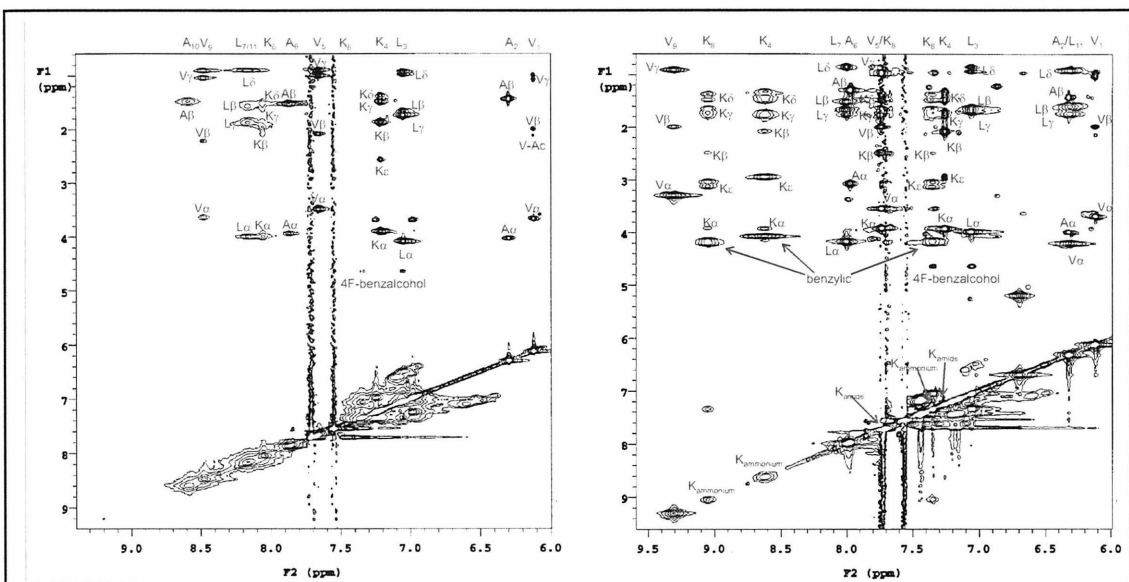


Figure 2.9: Differences in the tntocsy  $^1\text{H}$  NMR data for two samples of  $\text{b-Am}^{\text{F}}_{\text{P11}}$  in  $\text{CD}_2\text{Cl}_2$ .

In tntocsy NMR analysis, helical peptides are characterized by strong crosspeaks from sequential NN,  $\alpha\text{N}(i, i+3)$  and  $\alpha\beta(i, i+3)$  interactions (Fig.

2.10).<sup>12</sup> The tntocsy data from one  $\text{b-Am}^{\text{F}}_{\text{P11}}$  sample showed strong crosspeaks for all the

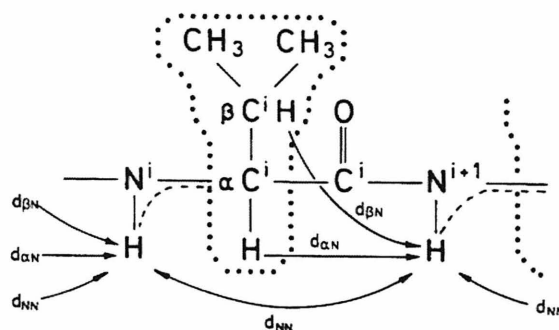


Figure 2.10: Crosspeaks seen in 2D NMR spectra of helical peptides. The dotted-line encloses an isolated spin system seen as through-bond coupling in TOCSY and COSY. The solid arrows denote through-space coupling seen in NOESY and ROESY analysis.

residues except those at the C-terminus. This data suggested that  $\text{b-Am}^{\text{F}}_{\text{P11}}$  had helical character in dichloromethane, but that the C-terminus was less structured than the rest of the peptide. The tntocsy spectra of the other two samples of  $\text{b-Am}^{\text{F}}_{\text{P11}}$  did not show any sequential NN,  $\alpha\text{N}(i, i+3)$  and  $\alpha\beta(i, i+3)$  crosspeaks.

Since the tnoesy experiments failed to yield data, wroesy experiments were run on those two samples. Strong crosspeaks were seen in the wroesy spectra, analysis of which suggested that these samples also had helical character. As before, the C-terminus was less structured than the rest of the peptide in these samples of **b-Am<sup>F</sup><sub>P11</sub>**.

Tnoesy experiments are useful for molecules that are either less than 1 kD or for larger molecules, while wroesy experiments are appropriate for molecules with a molecular weight around 2 kD. The molecular weight of **<sup>F</sup>P11<sup>2+</sup>** is 1.4 kD and that of **b-Am<sup>F</sup><sub>P11</sub>** is 3.1 kD. The BArF counterions are thought to be loosely associated with the peptide template, such that it should be tumbling in solution with an effective molecular weight around 1.4 kD. Therefore, the fact that the first sample of **b-Am<sup>F</sup><sub>P11</sub>** showed good NOESY peaks suggests that it was forming some sort of self-aggregate which boosted its molecular weight into the NOESY range. In contrast, the second samples had ROESY, and not NOESY, peaks. This suggests that these samples were monomeric in solution. The conformation of **b-Am<sup>F</sup><sub>P11</sub>** in dichloromethane is more complicated than the CD analysis in TFE would indicate.

#### **Pseudorotaxane Formation with M:**

The amount of **M** complexed with **DB24C8-CP** was evaluated by <sup>1</sup>H NMR in a variety of solvents,<sup>13</sup> at different temperatures, and with different ratios of **M** to crown-ether. Solvent had the largest influence on the amount of complex formed (**Table 2.4**), with the low dielectric solvents, chloroform and dichloromethane, promoting the highest amount of complexation – around 50% – and the high dielectric solvents, especially acetone and acetonitrile, allowing the least amount of complex to form. Surprisingly,

neither temperature (Table 2.5) nor the amount of **DB24C8-CP** added (Table 2.6) significantly influenced the amount of complex formed.

It was hypothesized that *para*-benzyl modification with an electron-withdrawing of an ammonium entity would increase its association in a pseudorotaxane complex. In agreement with this hypothesis, both **M-pOMe** and **M-pF** exhibited increased

Solvent	Dielectric Constant	Ammonium (%) Complexed	$K_a$ (L mol <sup>-1</sup> )
Chloroform	4.8	51	212
Dichloromethane	9.1	53	240
Nitromethane	39.4	39	105
Acetonitrile	37.5	25	44
Acetone	20.6	23	39

**Table 2.4:** Influence of solvent on complex of **M** to **DB24C8-CP** at r.t. in a solution an equimolar solution. 10mM solutions were analyzed by 600 MHz <sup>1</sup>H NMR.

Temperature (° C)	Ammonium (%) Complexed	$K_a$ (L mol <sup>-1</sup> )
-10.18	52	226
-0.17	51	212
20.15	51	212
30.13	51	212
40.06	51	212

**Table 2.5:** Influence of temperature on an equimolar complex of **M** to **DB24C8-CP** in d-chloroform.

Equivalentents of <b>DB24C8-CP</b>	Ammonium (%) Complexed
1.0	51
1.5	57
2.0	48
2.5	48
3.0	45

**Table 2.6:** Influence of increasing amounts of **DB24C8-CP** on complex with **M** (10mM) in d-chloroform at r.t.

complexation compared to the unmodified **M**. This trend correlated with the respective electron-withdrawing capabilities of the *para*-modifications (**Table 2.7**). The fluorine modification confers strong inductive withdrawal, and accordingly **M-pF** exhibited the highest association constant. (As an aside, the fluorine modification also serves as a useful tag for NMR studies.) The methoxy modification also provides inductive withdrawal, though a slightly less well, but has an additional, weak electron-donating capabilities through hyperconjugation that reduces its electron-withdrawing property. Fittingly, **M-pOMe** shows less of an enhancement over **M**. The NMR peaks of free **M-pCN** could not be resolved from those of the pseudorotaxane complex, making the data challenging to interpret. Regardless, no noticeable improvement in association was observed for **M-pCN**.

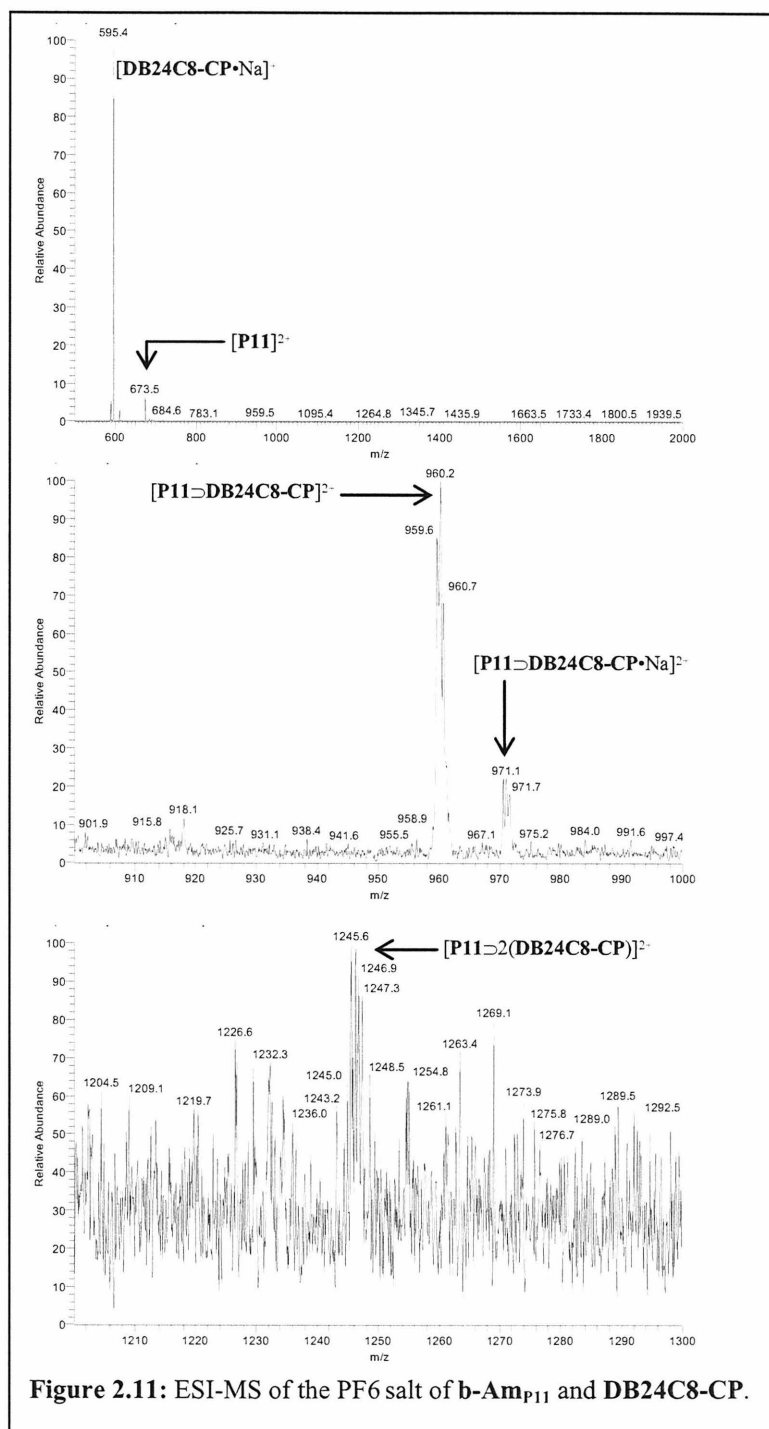
Ammonium Compound	(%) Complexed	$K_a$ (L mol <sup>-1</sup> )	$K_{rel}$
<b>M</b>	51	218	1.0
<b>M-pCN</b>	~39	~105	0.5
<b>M-pOMe</b>	63	460	2.1
<b>M-pF</b>	88	$6.11 \times 10^3$	28.0

**Table 2.7:** Influence of *para*-modification of the benzyl group on association constant. 10mM solutions in d-chloroform were analyzed by 600 MHz <sup>1</sup>H NMR.

### Mass Spectrometry Analysis of Pseudorotaxane Complex:

ESI-MS MS was used to analyze a solution containing the PF<sub>6</sub> salt of **P11**<sup>2+</sup> and **DB24C8-CP**. The [2]pseudorotaxane, [**P11**⊃**DB24C8-CP**], was detected, as was a small amount of the desired [3]pseudorotaxane, [**P11**⊃2(**DB24C8-CP**)] (**Fig. 2.11**). The weak signal of pseudorotaxanes compared to that of free **DB24C8-CP** and **P11** is likely due to the lack of soft ionization settings on the ESI mass spectrometer.<sup>14</sup> The spray voltage setting had to be raised drastically from the ideal setting for any signal to be seen,

thereby causing fragmentation of the complex within the instrument.



### NMR Analysis of the Pseudorotaxane Complexes:

The enhanced solubility of the BARF salt of **P11**, as compared to the PF<sub>6</sub> salt, allowed for <sup>1</sup>H NMR analysis of the pseudorotaxane formed between **P11** and **DB24C8-5en**. Formation of the complex decreases the inductive withdrawal of the crown-ether oxygen atoms, which is predicted to cause a small upfield shift in the DB24C8 methylene peaks.<sup>2</sup> Formation of the complex also increases the deshielding effect of the oxygen atoms, which is predicted to cause a significant downfield shift in the **P11** peaks. Previous studies with similar pseudorotaxane systems have demonstrated approximately 0.05 ppm upfield shifts for crown-ether protons and 0.5 to 1.0 ppm downfield shifts for the ammonium and benzylic methylene protons.<sup>3</sup>

The NMR spectra of free **b-Am<sub>P11</sub>** and **DB24C8-5en** were compared to the spectrum of a solution of the template with two equivalents of the crown-ether in d<sub>2</sub>-dichloromethane. Surprisingly, there were no obvious shifts of the crown-ether peaks in the spectrum of the complex compared to that of free **DB24C8-5en**. As expected, many of the template peaks were significantly shifted downfield. In particular, the ammonium protons – appearing as two peaks around 6.5 ppm in the spectrum of **b-Am<sub>P11</sub>** – were shifted downfield in the dual component sample such that they overlapped with one of the **DB24C8-5en** aromatic peaks at 7.0 ppm. In addition, the benzylic methylene protons of **P11** were shifted downfield so that they partially overlapped with a **DB24C8-5en** at 5.02 ppm. Because the shifted peptide peaks both overlapped with unshifted crown-ether peaks, the increase in integration values of the **DB24C8-5en** peaks were used to locate the shifted peptide protons in the spectrum of the complex. The **b-Am<sub>P11</sub>** peaks were shifted completely, indicating total generation of the [3]-pseudorotaxane.

No complex was observed between **b-Am<sub>P11</sub>** and **DB24C8-5en** in acetonitrile, nitromethane or nitromethane/chloroform because the peptide precipitated in each case. In the spectra collected in these solvents, only peaks arising from the crown molecule were observed.

<sup>19</sup>F NMR analysis of **b-Am<sup>F</sup><sub>P11</sub>** with two equivalents of **DB24C8-5en** also supported complete [3]-pseudorotaxane formation. Previous <sup>19</sup>F NMR analysis of **M-pF** established that the fluorine resonance shifts upfield by approximately 2

ppm upon binding **DB24C8-5en** (Fig.

**2.12**). In the spectrum of [**b-Am<sup>F</sup><sub>P11</sub>⊃2(DB24C8-5en)**], the two fluorine resonances are shift upfield by 1.7 and 2.1 ppm, respectively, as compared to those of **b-Am<sup>F</sup><sub>P11</sub>** (Fig. **2.13**). The NMR peaks of the [3]-pseudorotaxane are broader than those of the free **b-Am<sup>F</sup><sub>P11</sub>**, a difference that was also seen for the protons of the lysine residues in the <sup>1</sup>H spectra.

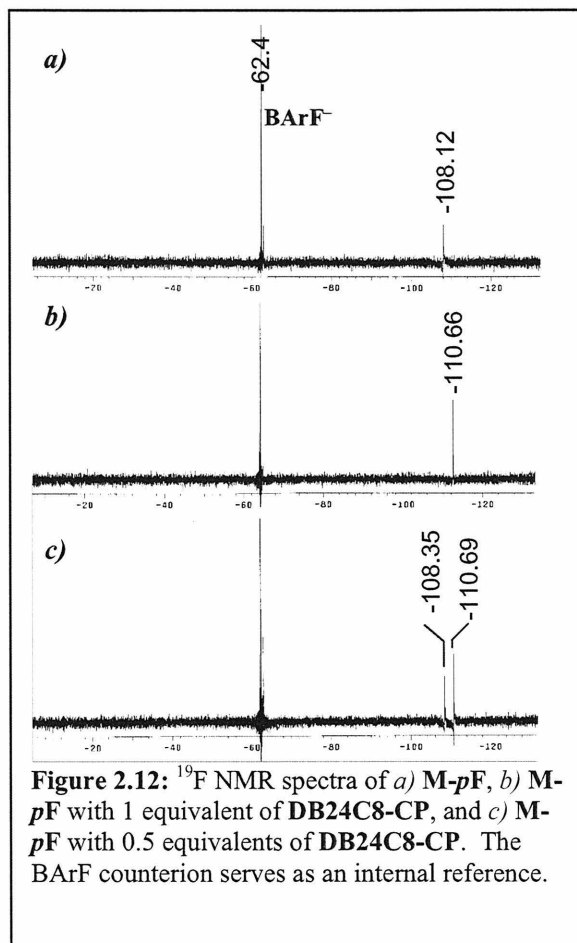


**Figure 2.12:** <sup>19</sup>F NMR spectra of a) **M-pF**, b) **M-pF** with 1 equivalent of **DB24C8-CP**, and c) **M-pF** with 0.5 equivalents of **DB24C8-CP**. The BArF counterion serves as an internal reference.

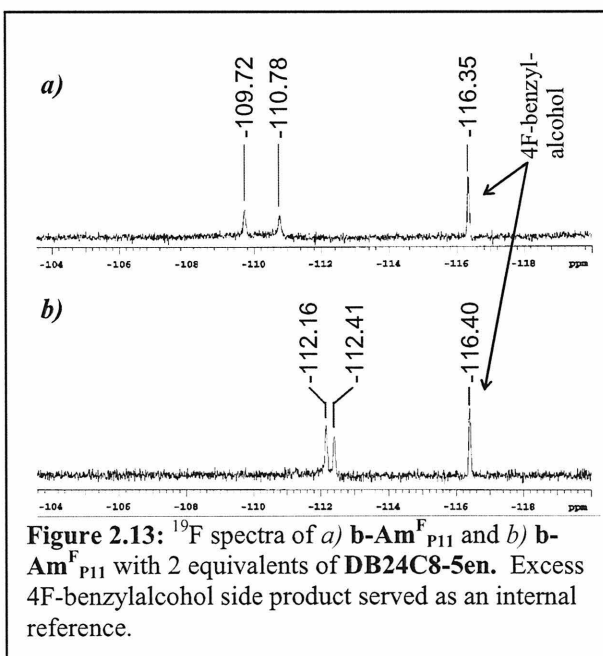


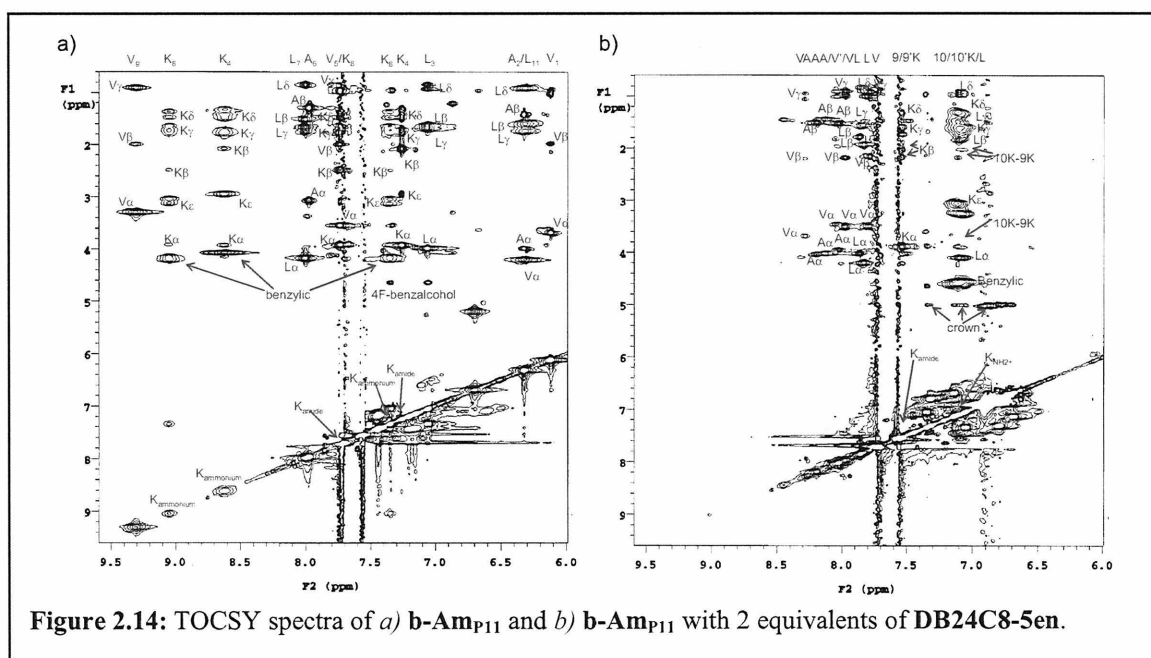
**Figure 2.13:** <sup>19</sup>F spectra of a) **b-Am<sup>F</sup><sub>P11</sub>** and b) **b-Am<sup>F</sup><sub>P11</sub>** with 2 equivalents of **DB24C8-5en**. Excess 4F-benzylalcohol side product served as an internal reference.

### NMR Analysis of Conformation of Pseudorotaxanes:

One of the samples of **b-Am<sup>F</sup><sub>P11</sub>** from the 2D NMR conformation studies was used to investigate the affect of adding crown ether on the conformation of the peptide. Tntocsy, tnnoesy and wroesy spectra were taken of a d<sub>2</sub>-dichloromethane solution containing **b-Am<sup>F</sup><sub>P11</sub>** and one equivalent of **DB24C8-5en**. No crosspeaks were observed in the wroesy spectrum, while some crosspeaks were observed in the tnnoesy experiment. Taken together, these data suggest that a higher molecular weight complex of [**b-Am<sup>F</sup><sub>P11</sub>⊃DB24C8-5en**] has formed. The NOE crosspeaks were fewer and weaker than those seen with free peptide, suggesting that forming the [3]-pseudorotaxane reduces the helical character of **b-Am<sup>F</sup><sub>P11</sub>**. In the tntocsy spectrum of the complex, the amide protons of the peptide converged. This is another indication of a less ordered structure. There were approximately two conformations identified in the tocsy spectrum, neither of which matched the spectrum of free **b-Am<sup>F</sup><sub>P11</sub>** or **b-Am<sup>F</sup><sub>P11</sub>** mixed with two equivalents of crown-ether (see below). This suggests the formation of two [2]-pseudorotaxanes, one with each ammonium center bound by one **DB24C8-5en**. The identities of the spin systems were determined, but because the tnnoesy data was weak, the connectivity was not.

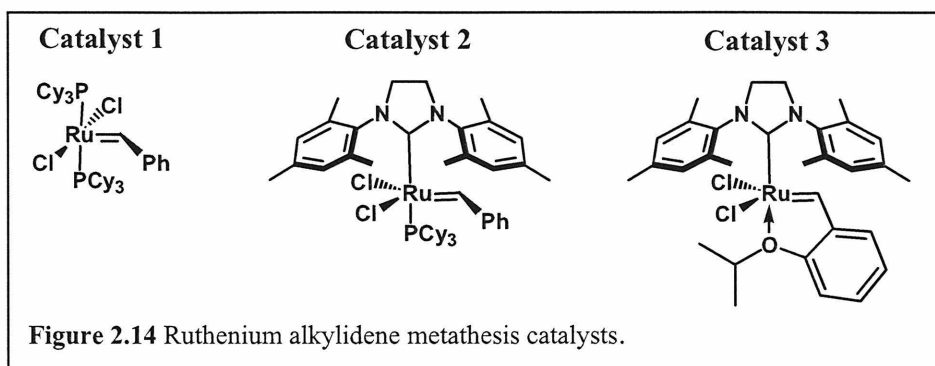
Another equivalent of **DB24C8-5en** was added to the sample and more 2D NMR data was gathered. Again, the wroesy failed to produce data. The NOE crosspeaks seen in the tnnoesy spectrum were similar in terms of intensity and number to those seen in the spectrum with one equivalent of **DB24C8-5en**. In the tntocsy spectrum, the amide protons converged even further, suggesting a further loss of structure (**Fig. 2.14**). Like residues – those of the same amino acid but at different positions in the sequence – had

amide and alpha protons with very similar chemical shifts. This is in contrast to those of free **b-Am<sup>F</sup><sub>P11</sub>**, which showed shifts that varied depending on the position of the residue within the peptide. In the spectrum with two equivalents of crown-ether, only one set of protons was observed for each amino acid and two for each of the ammonium spin systems. This indicated the presence of only one species, presumably the [3]-pseudorotaxane. Given the tnoesy data and the shifts of the amide protons, the complex likely adopts a random coil conformation.



### Binding Constants of **b-Am<sub>B</sub>**:

Isothermal titration calorimetry was used to find the association constants for [**b-Am<sub>B</sub>**⊃**DB24C8-5en**] and [**b-Am<sub>B</sub>**⊃**2(DB24C8-5en)**] in dichloromethane. The association constant,  $K_{a1}$ , for forming the one-to-one complex was  $4.53 \times 10^6 \text{ M}^{-1}$ , and the association constant,  $K_{a2}$ , for subsequently forming the one-to-two complex was  $7.17 \times 10^7 \text{ M}^{-1}$ . The relationship between  $K_{a1}$  and  $K_{a2}$  (i.e.,  $K_{a2}/K_{a1} > 0.25$ ) implies that there is positive cooperativity between the two binding sites.<sup>15-17</sup>



### Optimization of Metathesis Conditions

Three different alkylidene ruthenium metathesis catalysts<sup>18</sup> (**Fig. 2.15**) were studied to find the best one for the pseudorotaxane templation system. Cross metathesis reaction of **DB24C8-5en**, with or without the **b-Am<sub>B</sub>** template, were run with each of the three catalysts and the crude reaction mixtures were analyzed by HPLC. The results (**Table 2.8**) showed that catalyst **3** is most effective at achieving a balance between promoting dimerization and keeping the yield of the background reaction (i.e., without template) to a minimum. Interestingly, using 10 mol% **3** gave a 6.5-fold template enhancement over background, while using twice the amount of catalyst only gave a 2-fold enhancement.

<b>b-Am<sub>B</sub></b>	Catalyst	Yield (%) of Dimer
–	10 mol% <b>1</b>	12
+	10 mol% <b>1</b>	21
–	10 mol% <b>2</b>	22
+	10 mol% <b>2</b>	65
–	10 mol% <b>3</b>	6
+	10 mol% <b>3</b>	39
–	20 mol% <b>3</b>	26
+	20 mol% <b>3</b>	50

**Table 2.8:** A survey of metathesis catalysts. Reactions were run with 1mM **DB24C8-5en** at 40 °C.

A monomer with an olefin that is linked to the crown ether through an ether bond should be more electron rich, and therefore more reactive, than one attached via an ester bond. To test this theory, metathesis reactions were run with the ether-linked monomer, **DB24C8-e5en**. The results (**Table 2.9**) demonstrate that this monomer is more effective within the templation system than the ester-linked **DB24C8-5en**. Therefore, the crown-ether derivative for ADMET reactions (**DB24C8-diene**) was synthesized with ether-linked *n*-butene functionalities.

<b>b-Am<sub>B</sub></b>	Catalyst	Yield (%) of Dimer
–	10 mol% <b>2</b>	35
+	10 mol% <b>2</b>	72
–	25 mol% <b>3</b>	17
+	25 mol% <b>3</b>	78

**Table 2.9:** Reactions with 1mM **DB24C8-e5en** at 40 °C.

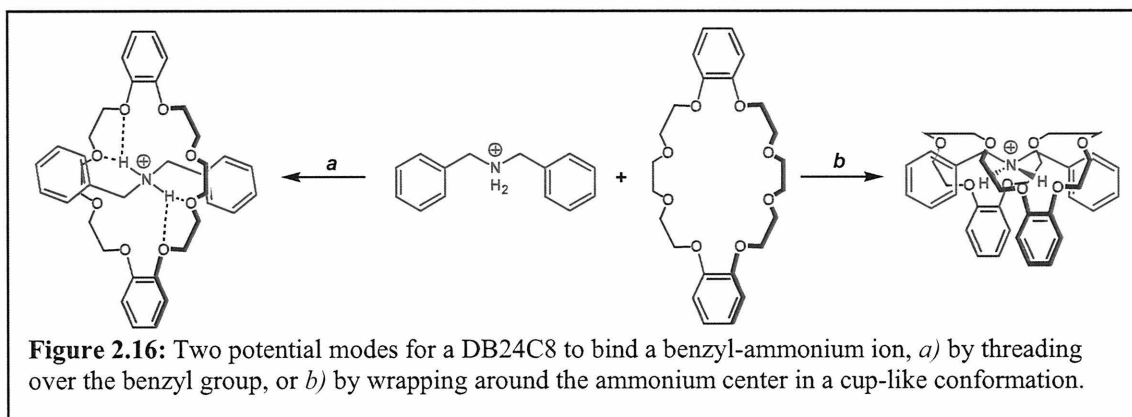
A continual problem in the metathesis reactions with the crown-ether monomers was the production of side-products arising from olefin isomerization. Addition of benzoquinone has been shown to reduce the amount of isomerization in ruthenium catalyzed metathesis reactions.<sup>19</sup> However, for this system (**Table 2.10**), the addition of benzoquinone did not reduce the amount of side-products generated nor did it significantly improve the yield of dimer. Therefore, benzoquinone was not used further.

Template	Catalyst	Benzoquinone	Yield (%) of Dimer
–	10 mol% <b>1</b>	–	12
–	10 mol% <b>1</b>	+	6
+	10 mol% <b>1</b>	–	21
+	10 mol% <b>1</b>	+	26
+	10 mol% <b>3</b>	–	38
+	10 mol% <b>3</b>	+	27

**Table 2.10:** The influence of benzoquinone on metathesis dimerization of 1mM **DB24C8-5en** at 40 °C.

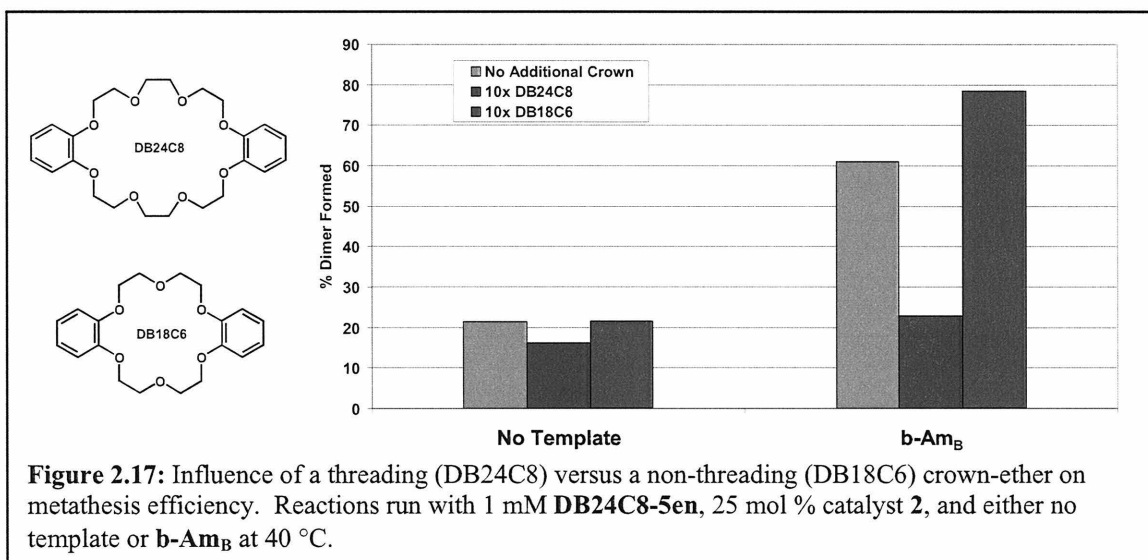
### Verification of [3]-Pseudorotaxane Formation:

There are two potential modes for a crown-ether to associate with an ammonium ion. In one mode, the crown-ether threads over the benzyl moiety (or other end-group) and encircles the ammonium center (**Fig. 2.16a**). The alternate “cupping” mechanism involves the crown-ether wrapping around the ammonium center without sliding over the end-group (**Fig. 2.16b**). Previous work with a stoppered dibenzyl ammonium ion has shown that threading is not necessary for significant shifts to be observed in  $^1\text{H}$  NMR spectra (Smidt, *S. unpublished*). The association due to a cupping conformation is undesirable for two reasons: first, it is a more transient type of interaction, and second, it is not specific for the DB24C8-sized crown ether.



To test the mode of association, metathesis reactions were run with addition of one of two different sized crown-ethers molecules without olefin modification. It was hypothesized that addition of unmodified DB24C8, a crown-ether large enough to bind the template ammonium center by threading over the benzyl functionality, would block DB24C8-5en from threading onto the template and thereby reduce template-directed metathesis due to a threading interaction. On the other hand, addition of unmodified DB18C6, a crown-ether too small to thread over the benzyl group, would only reduce

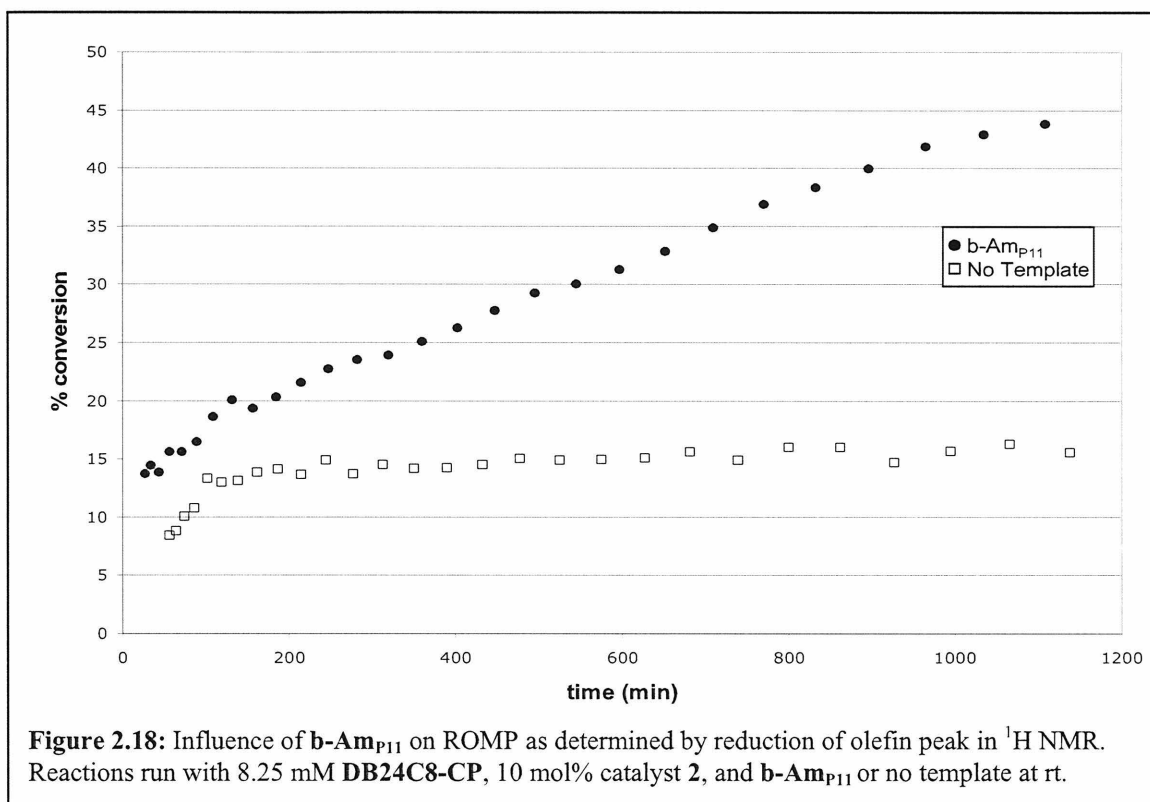
template-directed metathesis arising from a cup-like binding interaction. Analysis of the reactions by HPLC showed that addition of a large excess of DB24C8 had a minimal effect on the reaction without template, but drastically reduced the yield of the reaction containing template **b-Am<sub>B</sub>** (Fig. 2.17). On the other hand, addition of a large excess of DB18C6 had no influence on either reaction. Taken together these results verified that the desired [3]-pseudorotaxane metathesis complex was forming.



### **b-Am<sub>P11</sub>** Influence on ROMP of DB24C8-CP:

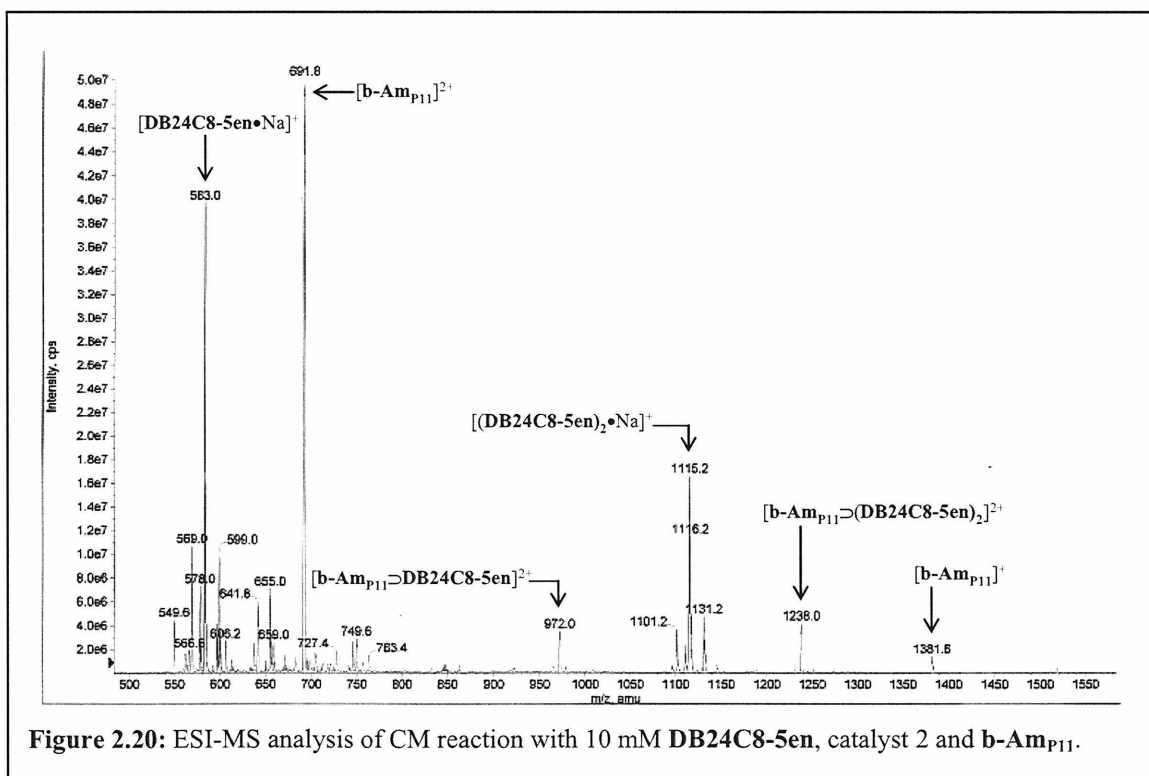
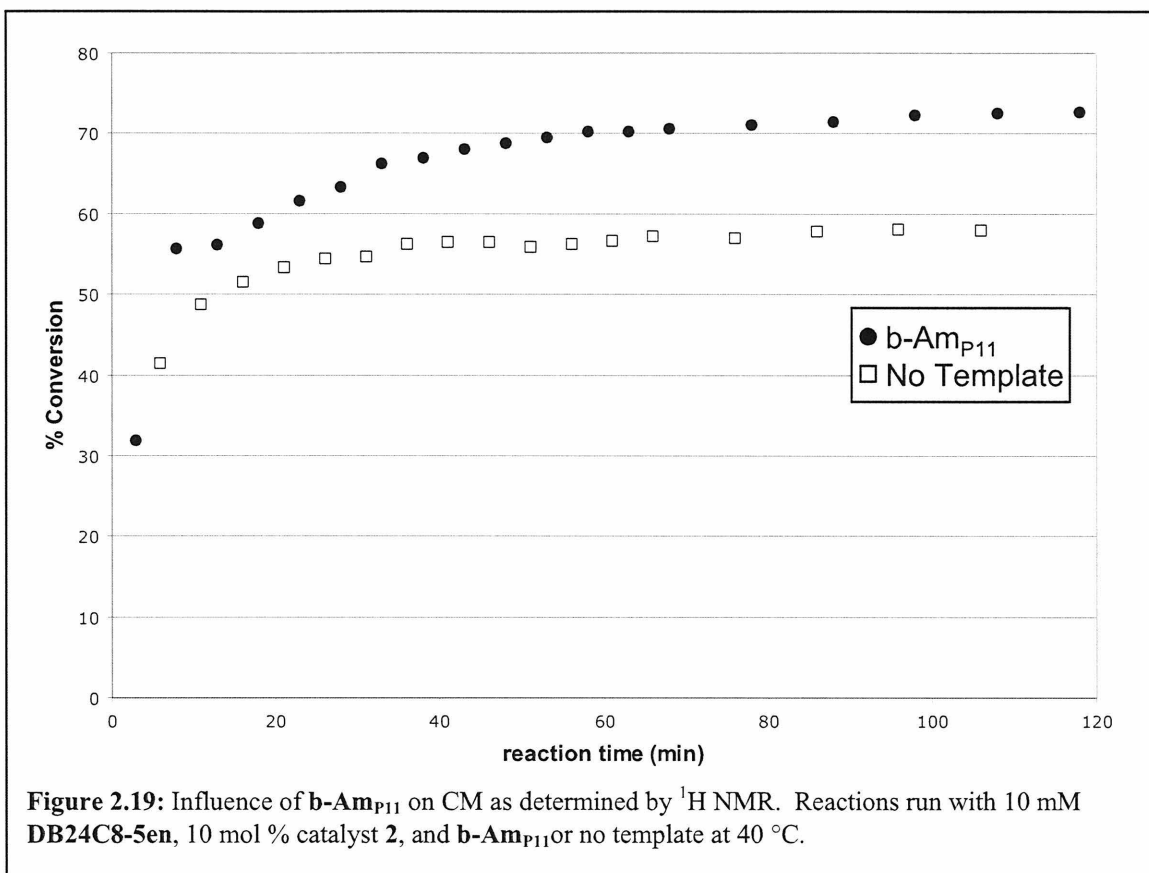
<sup>1</sup>H NMR spectroscopy was used to follow a ROMP reaction of **DB24C8-CP** in the presence and absence of the **b-Am<sub>P11</sub>** template. The reaction was run at a concentration of crown-ether monomer less than 10 mM to stay significantly below (90 times) the critical concentration needed for ROMP to proceed in solution. The reaction of [**b-Am<sub>P11</sub>**⊃**2(DB24C8-CP)**] using catalyst **2** was established to be almost 45% complete within 16 hours, whereas the reaction of **DB24C8-CP** in the absence of the template **b-Am<sub>P11</sub>** resulted in less than 15% conversion under identical reaction conditions in the same amount of time (Fig. 2.18). The template also influenced the rate

of the reaction. In the presence of **b-Am<sub>P11</sub>**, ROMP of the monomer occurred faster than in the absence of template.



### Influence of **b-Am<sub>P11</sub>** on Cross Metathesis:

Cross metathesis reactions of **DB24C8-5en** (10 mM) using catalyst **2** with and without template **b-Am<sub>P11</sub>** were monitored by <sup>1</sup>H NMR. As with the ROMP experiment, the template enhanced both the rate and yield of the dimerization (**Fig. 2.19**). The reaction of [**b-Am<sub>P11</sub>**⊃**2(DB24C8-5en)**] was greater than 70% complete in 80 minutes, while the reaction of **DB24C8-5en** without template was only 57% within the same amount of time.



Aliquots of both reactions were analyzed by ESI-MS. Peaks arising from the **DB24C8-5en** starting material and dimer product were visible in both spectra. In the spectrum (Fig. 2.20) of the reaction mixture with **b-Am<sub>P11</sub>**, there were also peaks from **b-Am<sub>P11</sub>**, a doubly charged ions for two [2]-pseudorotaxanes: [**b-Am<sub>P11</sub>⊃DB24C8-5en**] and [**b-Am<sub>P11</sub>⊃(DB24C8-5en)<sub>2</sub>**].

#### **Influence of b-Am<sub>B</sub> on Cross Metathesis:**

The same cross metathesis experiment was run using template **b-Am<sub>B</sub>**.<sup>7</sup> The dimerization of [**b-Am<sub>B</sub>⊃2(DB24C8-5en)**] was established to be 73% complete within 40 minutes, whereas the dimerization of **DB24C8-5en** in the absence of the template resulted in only 48% conversion in the same amount of time. The template also influenced the rate of the reaction. In the presence of **b-Am<sub>B</sub>**, cross metathesis of **DB24C8-5en** occurred faster than in the absence of template.

#### **Comparison of Templates for Cross Metathesis:**

The first three bis-ammonium peptide templates, **b-Am<sub>P11</sub>**, **b-Am<sub>P18</sub>** and **b-Am<sub>P20</sub>**, were compared to the linear template **b-Am<sub>B</sub>** (Table 2.11), which had previously been shown to significantly influence cross metathesis with the templation system. In a 2 hour metathesis reaction of **DB24C8-5en**, **b-Am<sub>B</sub>** showed almost a three-fold enhancement in dimerization compared to the background reaction. On the other hand, the three peptide template had almost no influence on the yield of dimer. From these results it can be concluded that **b-Am<sub>B</sub>** promotes dimer formation, while peptide templates **b-Am<sub>P11</sub>**, **b-Am<sub>P18</sub>** and **b-Am<sub>P20</sub>** do not.

Template	Yield (%) of Dimer	Enhancement over background
–	23	–
<b>b-Am<sub>B</sub></b>	65	2.8
<b>b-Am<sub>P11</sub></b>	31	1.3
<b>b-Am<sub>P18</sub></b>	25	1.1
<b>b-Am<sub>P20</sub></b>	27	1.2

**Table 2.11:** Comparison of bis-ammonium templates in cross metathesis reactions using 10 mol% **2** and 1mM **DB24C8-5en** at 40 °C.

### Comparison of Templates for ADMET Dimerization:

ADMET reactions were carried out using the bis-ammonium templates and catalysts **2** and **3** (Table 2.12). A very high background reaction yield was seen in the reactions with catalyst **2**, but was reduced when the concentration of **DB24C8-diene** was reduced by half. Using this catalyst, **b-Am<sub>B</sub>** showed a template-directed enhancement of dimer yield at both concentrations of monomer, although the effect was more pronounced at the lower concentration. On the other hand, there was only a minimal template effected observed for **b-Am<sub>P11</sub>**.

**Table 2.12:** Comparison of different templates and different catalyst in ADMET reactions with 1mM **DB24C8-diene** at 40 °C.

Template	Catalyst	Yield (%) of Dimer
–	10 mol% <b>2</b>	56
<b>B</b>	10 mol% <b>2</b>	76
–	10 mol% <b>2</b>	34*
<b>B</b>	10 mol% <b>2</b>	72*
–	10 mol% <b>2</b>	58
<b>P<sub>11</sub></b>	10 mol% <b>2</b>	66
–	25 mol% <b>3</b>	33
<b>B</b>	25 mol% <b>3</b>	87
<b>P<sub>3</sub></b>	25 mol% <b>3</b>	85

\* [DB24C8-diene] = 0.5mM

Using catalyst **3** significantly reduced the background reaction seen with catalyst **2**. The templates **b-Am<sub>B</sub>** and **b-Am<sub>P3</sub>** were found to be equally effective with this catalyst, effecting close to a three-fold enhancement in dimer yield over background.

#### Metathesis Dimerization with the **b-Am<sub>A</sub>** Templates:

The series of alkane-linked bis-ammonium templates, **b-Am<sub>A4</sub>** through **b-Am<sub>A12</sub>**, was used to assess the influence of template rigidity on the ability of a template to promote metathesis. Comparison of the metathesis reactions with the alkane-templates to those with the rigid template **b-Am<sub>B</sub>** showed that increasing the flexibility of the template did not compromise template efficacy (**Table 2.13**). All of the **b-Am<sub>A</sub>** templates gave significantly higher dimerization yields than the background reaction, and as high, or higher, than the rigid template **b-Am<sub>B</sub>**. In addition, within the range studied there was no correlation between linker length and template efficacy. However, it is likely distance dependence would be seen with increasingly long spacing between binding sites, an experiment that was beyond the scope of this study.

Template	Yield (%) of Dimer
<b>b-Am<sub>A4</sub></b>	63
<b>b-Am<sub>A5</sub></b>	61
<b>b-Am<sub>A6</sub></b>	68
<b>b-Am<sub>A8</sub></b>	60
<b>b-Am<sub>A10</sub></b>	63
<b>b-Am<sub>A12</sub></b>	66
<b>b-Am<sub>B</sub></b>	52
–	25

**Table 2.13:** Influence of linear templates on ADMET dimerization. Reactions were run with 1mM **DB24C8-diene** and 20 mol% **3** at 40 °C.

### Template Purification:

One distinct difference between the effective templates and the ineffective ones was their purity. The peptides **P11**, **P18** and **P20** could not be purified after the reductive amination reaction, and they were the least effective templates. On the other hand, **P3**, **B** and the **A**-series were all purified prior to their use as templates, and they all significantly enhanced the yield of metathesis dimerization. To investigate this apparent correlation between efficacy and purity, **b-Am<sub>A6</sub>** was synthesized without purification after the benzyl protection. As with the peptides, selective mono-benzyl protection of each amine functionality was confirmed by MS.

It was found that template purification had a significant impact on the ability of **b-Am<sub>A6</sub>** to influence metathesis dimerization (**Table 2.14**). Comparison of the same template with and without purification shows that purification increased the dimer yield by 50%.

Template	Yield (%) of Dimer
<b>b-Am<sub>A6</sub></b>	78
Crude <b>b-Am<sub>A6</sub></b>	39
–	21

**Table 2.14:** Influence of template purity on metathesis dimerization. Reactions were run with 1mM **DB24C8-diene** and 20 mol% **3** at 40 °C.

### ADMET Trimerization:

In all of the ADMET dimerization reactions no trimer or longer products were observed by HPLC or mass spec analysis. This suggests that a 1 mM concentration of monomer is not high enough to allow polymerization to occur. However, if the template motifs can be extended beyond dimerization, the addition of a tris-ammonium template should promote the formation of trimer products.

Template	Yield (%) Dimer	Yield (%) Trimer
–	28	0
<b>t-Am<sub>P15</sub></b>	31	0
<b>t-Am<sub>P5</sub></b>	58	19

**Table 2.15:** Template-directed metathesis trimerization. Reactions were run with 1mM **DB24C8-diene** and 20 mol% **3** at 40 °C.

Neither the control reaction nor the reaction with **t-Am<sub>P15</sub>**, a template that was not purified, yielded any trimer product. The **t-Am<sub>P15</sub>** template did enhance the metathesis yield compared to background. However, the yield of trimer was modest and most of the product formed was dimer. Analysis of the dimer and trimer products showed them to be cyclic – arising from a final intramolecular metathesis reaction to close the molecule on itself.

### III. Conclusions

The series of experiments outlined above was designed to study the suitability of the pseudorotaxane binding motif for a template-directed metathesis polymerization system. A peptide template, **bAm<sub>P3</sub>**, was identified that was as effective as the control linear templates at enhancing metathesis dimerization. It was also discovered that template rigidity and defined structure are not necessary to promote metathesis dimerization, although they may be important for longer polymerization reactions.

The successful bis-ammonium peptide template design did not extend to the tris-ammonium template. While **t-Am<sub>P5</sub>** was able to influence the overall yield of the metathesis reaction, the majority of the product formed was the cyclic dimer. It was hypothesized that a stronger non-covalent or a covalent recognition motif might aid in the synthesis of oligomers larger than dimers.

## IV. Experimental

### General:

The peptide starting materials for template **b-Am<sub>P11</sub>** and **t-Am<sub>P15</sub>** were synthesized by the Biopolymer Synthesis and Analysis Facility at the California Institute of Technology and was used without further purification. The peptide starting materials for templates **b-Am<sub>P18</sub>**, **b-Am<sub>P20</sub>**, and **b-Am<sub>P3</sub>** were synthesized by the GenScript Corporation. The peptide starting material for **b-Am<sub>P3</sub>** was also purified to 97% by GenScript. All chemicals were obtained from commercial sources and used as received. Deuterated NMR solvents were from Cambridge Isotopes.

<sup>1</sup>H-NMR spectra were recorded on Varian 300 or 500 MHz NMR. Electrospray ionization (ESI) and MALDI mass spectrometry were performed at the Mass Spectrometry Center in the Department of Chemistry at the California Institute of Technology. Circular dichromism (CD) spectra were recorded on an AVIV CD spectrometer, model 62DS.

### Synthesis of b-Am<sub>P11</sub>, b-Am<sub>P18</sub>, and b-Am<sub>P20</sub> Templates:

**Benylation:** The peptide starting material was dissolved in trifluoroethanol (TFE) and 1M aq. NaOH. Benzaldehyde (2 equivalents) was added and the solution was stirred for 20 min. Sodium borohydride (4 equivalents) was added and the solution was stirred for 30 min. Consecutive additions of benzaldehyde and sodium borohydride were repeated two more times, at which point MALDI-MS analysis confirmed the reaction was complete. A small amount of acetone was added to the solution to quench excess NaBH<sub>4</sub>. The reaction was diluted with chloroform and washed with water (2x). The organic layer was dried over Na<sub>2</sub>SO<sub>4</sub> and concentrated to yield the benzyl-modified product.<sup>20</sup>

**P11:** 10.0 mg of peptide Ac-VALKVALKVAL-NH<sub>2</sub> (0.00858 mmol) in 500 μL of TFE and 50 μL of 1M NaOH (aq.) yielded 10.7 mg of product (93%): MALDI-MS (*m/z*) 1346 [M + H]<sup>+</sup>, 1369 [M + Na]<sup>+</sup>.

**P15<sup>F</sup>:** 13.3 mg of peptide Ac-VALKVALKVALKVAL-NH<sub>2</sub> (0.00843 mmol) in 700 μL of TFE and 10 μL of 1M NaOH (aq.) yielded 14.4 mg of product (90%): MALDI-MS (*m/z*) 1902 [M + H]<sup>+</sup>, 1924 [M + Na]<sup>+</sup>.

**P18<sup>F</sup>:** 10.0 mg of peptide Ac-LALLALKLALAKLALLAL-NH<sub>2</sub> (5.34 μmol) in 500 μL of TFE and 10 μL of 1M NaOH (aq.) yielded 5.6 mg of product (50%): MALDI-MS (*m/z*) 2091 [M + H]<sup>+</sup>, 2113 [M + Na]<sup>+</sup>.

**P20<sup>F</sup>:** 10.0 mg of peptide Ac-VALVALKVALVALKVALVAL-NH<sub>2</sub> (4.96 μmol) in 500 μL of TFE and 10 μL of 1M NaOH (aq.) yielded 7.8 mg of product (70%): MALDI-MS (*m/z*) 2233 [M + H]<sup>+</sup>, 2255 [M + Na]<sup>+</sup>.

**P11<sup>2+</sup>·(PF<sub>6</sub><sup>-</sup>)<sub>2</sub>:** P11 (23.2 mg, 0.0172 mmol) was dissolved in 1 mL of TFE, and a 60 wt % solution of HPF<sub>6</sub> in water (20.9 μL, 0.086 mmol) was added dropwise. The solution

was stirred for 2 hours and then concentrated to give a clear gel. Addition of water caused precipitation of a white solid, which was isolated by filtration. The solid was washed with water (2x), then ether (2x). It was collected and dried over night to give the desired product (16.1 mg, 57%): ESI-MS ( $m/z$ ) 674  $[M + 2H]^{2+}$ .

**$[H(Et_2O)_2]^+[BArF]^-$** : A 0.045M solution of NaBArF (49.7 mg, 0.0561 mmol) in anhydrous  $Et_2O$  was dried over 4 angstrom molecular sieves for 12 hr. The solution was cooled on ice, and 1M HCl in anhydrous  $Et_2O$  was added dropwise. The solution was allowed to sit under argon on ice for 1.5 hr, during which time it turned cloudy as NaCl precipitated. The solution was filtered through a 0.45 $\mu$ m PFTE filter and concentrated to give a white solid. At all times, the reaction and product were kept on ice.

**b-Am<sub>P11</sub>**: **P11** (13.4 mg, 0.00996 mmol) was cooled on ice under argon. A 0.1M solution of  $[H(Et_2O)_2]^+[BArF]^-$  in anhydrous  $Et_2O$  (199.0  $\mu$ L) was added. The material was dissolved/suspended in 800  $\mu$ L anhydrous  $Et_2O$ , and was stirred on ice for 1.5 hr. The reaction was concentrated, and the material was taken up in DCM. The solution was filtered to remove the insoluble particulate, and re-concentrated to yield the desired product (14.0 mg, 46%): ESI-MS ( $m/z$ ) 674  $[M + 2H]^{2+}$ , 863  $[BArF]^-$ .

**b-Am<sub>P11</sub><sup>F</sup>**: The same procedure was used as for **b-Am<sub>P11</sub>**, but starting with **P11<sup>F</sup>** (17.1 mg, 0.0124 mmol) and yielding 18.9 mg product (49%).

**t-Am<sub>P15</sub><sup>F</sup>**: The same procedure was used as for **b-Am<sub>P11</sub>**, but starting with **P15<sup>F</sup>** (5.0 mg, 2.63  $\mu$ mol) and yielding 8.0 mg product (68%), the identity of which was confirmed by <sup>1</sup>H NMR.

**b-Am<sub>P18</sub><sup>F</sup>**: The same procedure was used as for **b-Am<sub>P11</sub>**, but starting with **P18<sup>F</sup>** (5.6 mg, 2.68  $\mu$ mol) and yielding 7.4 mg product (72%).

**b-Am<sub>P20</sub><sup>F</sup>**: The same procedure was used as for **b-Am<sub>P11</sub>**, but starting with **P20<sup>F</sup>** (7.8 mg, 3.49  $\mu$ mol) and yielding 8.3 mg product (60%).

### Synthesis of b-Am<sub>P3</sub> and t-Am<sub>P5</sub>:

**Solid-phase Synthesis of Peptide Starting Materials:** The peptide starting materials Ac-KAK-NH<sub>2</sub> and Ac-KAKAK-NH<sub>2</sub> were synthesized using standard Fmoc chemistry on Rink Amide MBHA resin from Novabiochem. During the synthesis, Fmoc deprotection was achieved with 20% piperidine in DMF. Amino acid coupling was achieved using the coupling reagents HOBt and DIPCDI in DMF. After the final Fmoc deprotection, the N-terminus was acetylated using acetic anhydride and DIEA in DMF. Lysine deprotection and peptide cleavage were achieved using a solution of TFA and TIS in water. After cleavage, the peptides were precipitated with cold ethyl ether, isolated by filtration, dissolved in MeOH and concentrated. The identity of each peptide was confirmed by <sup>1</sup>H NMR and ESI MS.

**Benylation:** The peptide was dried under vacuum in a flame-dried flask overnight. An oven-dried stirbar and activated 4 Å molecular sieves were added to the flask under argon. The peptide was dissolved in anhydrous methanol and allowed to stir under argon for approximately 20 minutes. Benzaldehyde (6 equivalents) was added to the solution. The reaction was allowed to stir for 30 minutes, and then the solvent was removed under vacuum. The material was dried under vacuum for at least 2 hours to try to remove as much unreacted benzaldehyde as possible. The material was redissolved in anhydrous methanol and sodium borohydride (12 equivalents) was added. After stirring for 30 minutes, excess reducing agent was quenched with acetone and the reaction was concentrated. The reaction was dissolved in ethyl acetate and washed with water (3x), dried and concentrated. The crude material was dissolved in 9:1 0.1% TFA (aq):CH<sub>3</sub>CN, with the addition of extra CH<sub>3</sub>CN to allow complete dissolution. The material was then purified by HPLC on a C18 reverse phase column, using a gradient from 10% to 100% CH<sub>3</sub>CN in 0.1% TFA (aq). The run was monitored by UV at 250 nm. The desired product was collected and concentrated as the TFA-salt. <sup>1</sup>H NMR and ESI-MS were used to verify the product identity.

**P3:** 35.5 mg of peptide Ac-KAK-NH<sub>2</sub> (0.0919 mmol) yield 14.7 mg of product as a TFA-salt (28%).

**P5:** 45.0 mg of peptide Ac-KAKAK-NH<sub>2</sub> (0.0768 mmol) yielded 7.0 mg of product as a TFA-salt (11%).

**Generation of BARF-salt:** The TFA-salt of benzylated peptide was dissolved in a minimal amount of water. Dichloromethane was added to make a biphasic solution. Two or three equivalents of NaBARF were added to the solution. The solution was stirred vigorously for 12 hours. The organic layer was separated, washed with water (2x), dried and concentrated. <sup>1</sup>H NMR was used to verify the correct ratio of peptide to ion.

**b-Am<sub>P3</sub>:** 3.4 mg of the TFA-salt of **P3** (4.28 μmol) yield 7.8 mg of product (79%).

**t-Am<sub>P5</sub>:** 7.0 mg of the TFA-salt of **P5** (5.84 μmol) yielded 16.0 mg of product (79%).

### **Synthesis of b-Am<sub>A</sub> Series:**

The series of alkyl linked bisammonium templates was synthesized from commercially available alkyl-diamine reagents using standard reductive amination conditions. Each alkyl-diamine was dissolved in anhydrous MeOH to a concentration of 1M, and 2.2 equivalents of benzaldehyde was added. After stirring for 30 min., 4.4 equivalents of NaBH<sub>4</sub> was added. The reaction was stirred for at least 1 hr, and excess reducing agent was quenched with acetone. The reaction was diluted with EtOAc, washed with water (2x) and then with sat. brine (2x), dried over Na<sub>2</sub>SO<sub>4</sub> and concentrated. Purification by silica gel column chromatography yielded pure dibenzyl-protected product. The dibenzyl amines were protonated with HCl, and the resulting HCl-salt precipitate was isolated. Then, the chloride counterion was replaced by the BARF counterion in a biphasic solution

of dichloromethane and water using 2 equivalents of NaBARF.  $^1\text{H}$  NMR was used to confirm the correct template to counterion ratio.

### **Synthesis of M, M-*p*F, M-*p*OMe, M-*p*CN:**

***O*-TBDPS-butanol-4-amine:** Butanol-4-amine (200.0 mg, 2.244 mmol) was dissolved in 1.8 mL anhydrous DMF. Imidazole (3.366 mmol) was added, then TBDPSCI (2.468 mmol) was added dropwise. The reaction was complete in 4 hr, as judged by TLC. Removal of the solvent terminated the reaction, and the crude material was used without further purification.

***O*-TBDPS-butanol-4-benzylamine:** Crude ***O*-TBDPS-butanol-4-amine** (1.122 mmol) was dissolved in methanol, and the pH was taken to 8.5 with 0.5 mL of 1.0 M NaOH. Benzaldehyde (2.244 mmol) was added and the solution was stirred for thirty min at rt.  $\text{NaBH}_4$  (4.488 mmol) was added, causing the evolution of gas, and the reaction was stirred for thirty min. The consecutive additions of benzaldehyde and  $\text{NaBH}_4$  were repeated one more time, with thirty min of stirring after each addition. At that point, TLC showed that **1** had been consumed. Excess  $\text{NaBH}_4$  was quenched with acetone and the reaction was concentrated. The residue was taken up in EtOAc and washed with water (2x). The organic layer was dried over  $\text{Na}_2\text{SO}_4$  and concentrated. The crude material was purified by silica gel column chromatography in 1:1 EtOAc:Hex to yield pure material (231.9 mg, 50%): ESI-MS ( $m/z$ ) 418  $[\text{M} + \text{H}]^+$ .

**M:** 231.9 mg of ***O*-TBDPS-butanol-4-benzylamine** (0.555 mmol) was dissolved in methanol. 6.05M HCl was added to give a pH 2.5 solution, which was stirred at rt for 3 hr. The reaction was concentrated and the residue was taken up in biphasic solution of water and  $\text{CHCl}_3$ , and NaBARF (<0.555 mmol) was added batch-wise with vigorous shaking after each addition until it no longer went into solution immediately. The organic layer was separated, dried over  $\text{Na}_2\text{SO}_4$  and concentrated to yield product with the correct 1:1  $\text{M}^+$  to  $\text{BARF}^-$  ratio (534.6 mg, 75%).

***O*-TBDPS-butanol-4-*p*Fluorobenzylamine:** The same procedure was used as for ***O*-TBDPS-butanol-4-benzylamine**, replacing benzaldehyde with 4-fluorobenzaldehyde. A reaction with 100 mg ***O*-TBDPS-butanol-4-amine** (0.305 mmol) yielded 33.4 mg pure product (25%): ESI-MS ( $m/z$ ) 436  $[\text{M} + \text{H}]^+$ .

***O*-TBDPS-butanol-4-*p*Methoxybenzylamine:** The same procedure was used as for ***O*-TBDPS-butanol-4-benzylamine**, replacing benzaldehyde with 4-methoxybenzaldehyde. A reaction with 100 mg ***O*-TBDPS-butanol-4-amine** (0.305 mmol) yielded 70.0 mg pure product (51%): ESI-MS ( $m/z$ ) 448  $[\text{M} + \text{H}]^+$ .

***O*-TBDPS-butanol-4-*p*Cyanobenzylamine:** The same procedure was used as for ***O*-TBDPS-butanol-4-benzylamine**, replacing benzaldehyde with 4-cyanobenzaldehyde. A reaction with 100 mg ***O*-TBDPS-butanol-4-amine** (0.305 mmol) yielded 3.4 mg pure product (3%): ESI-MS ( $m/z$ ) 443  $[\text{M} + \text{H}]^+$ .

**M-pF:** The same procedure was used as for **M**, but starting with **O-TBDPS-butanol-4-pFluorobenzylamine** (55.0 mg, 0.126 mmol), to yield 110.0 mg product (67%).

**M-pOMe:** The same procedure was used as for **M**, but starting with **O-TBDPS-butanol-4-pMethoxybenzylamine** (70.0 mg, 0.126 mmol), to yield 98.0 mg product (55%).

**M-pCN:** The same procedure was used as for **Model**, but starting with **O-TBDPS-butanol-4-pCyanobenzylamine** (3.4 mg, 0.00768 mmol), to yield 8.4 mg of product (84%).

### **Synthesis of DB24C8-derivatives:**

**ADMET diene:** The hydroxyl functionalities of methyl 3,5-dihydroxybenzoate were alkylated using 1-bromobutene and  $K_2CO_3$ . The resulting compound was saponified using potassium hydroxide in a water and ethanol solution to give the desired diolefin acid compound.

**Representative Synthesis of Ester-linked DB24C8-Derivatives:** EDC (1.36 mmol) was added to a stirring solution of the carboxylic acid derivative (1.36 mmol) and a few crystals of DMAP in DCM (10 mL), followed by the addition of **DB24C8-OH** (1.04 mmol). The reaction mixture was allowed to stir at ambient temperature for 16 hr, before removing the solvent *in vacuo*. Purification by silica gel column chromatography (2% MeOH/DCM) afforded each product as a white solid.

**DB24C8-5en:**  $^1H$  NMR (500 MHz,  $CD_2Cl_2$ )  $\delta$  = 2.32–2.38 (m, 2H), 2.40–2.44 (m, 2 H), 3.75 (s, 8H), 3.83–3.86 (m, 8 H), 4.09–4.12 (m, 8H), 5.01 (s, 2H), 4.96–5.06 (m, 2H), 5.79–5.85 (m, 1H), 6.82–6.86 (m, 7H);  $^{13}C$  NMR (125 MHz,  $CDCl_3$ )  $\delta$  = 28.7, 33.4, 66.1, 69.3, 69.4, 69.7, 69.8, 71.19, 71.22, 113.4, 114.2, 115.4, 121.3, 121.6, 128.9, 136.5, 148.7, 148.8, 172.8; MALDI-ICR:  $[C_{30}H_{40}O_{10}Na]^+$  = 583.2515, calcd = 583.2519.

**DB24C8-diene:**  $^1H$  NMR (300 MHz,  $CDCl_3$ )  $\delta$  = 2.58 (dt, 4H), 3.85 (s, 8H), 3.91–3.98 (m, 8H), 4.06 (t, 4H), 4.12–4.20 (m, 8H), 5.08–5.30 (m, 6H), 5.82–5.91 (m, 2H), 6.62 (s, 1H), 6.78–7.0 (m, 7H), 7.19 (s, 2H); HRFAB:  $[C_{40}H_{50}O_{12}Na]^+$  = 722.3338, calcd 722.3303.

**DB24C8-e5en:** A solution of **DB24C8-OH** (2.0 g, 4.2 mmol) in THF (40 mL) was slowly added dropwise to a suspension of NaH (60% in oil, 252 mg, 10.5 mmol) in THF (40 mL). This mixture was stirred at ambient temperature under an  $N_2$  atmosphere until no further  $H_2$  evolution was observed. The mixture was cooled with an ice bath and a solution of 5-bromopentene (934 mg, 6.3 mmol) in THF (40 mL) was added dropwise. The reaction was stirred 2 days under ambient conditions and subsequently quenched with isopropanol, and then with water. All solvents were removed under reduced pressure and the residue purified by silica gel column chromatography with EtOAc to give the desired product (1.44 g, 63%) as a white solid:  $^1H$  NMR (300 MHz,  $CDCl_3$ )  $\delta$  = 1.61–1.80 (m, 2H), 2.14–2.20 (m, 2H), 3.43 (t, 2H), 3.82 (s, 8H), 3.83–3.89 (m, 8H), 4.07–4.09

(m, 8H), 4.41 (s, 2H), 4.93–5.03 (m, 2H), 5.71–5.88 (m, 1H), 6.80–6.91 (m, 7H);  $^{13}\text{C}$  NMR (125 MHz,  $\text{CDCl}_3$ )  $\delta$  = 28.9, 30.2, 69.0, 69.4, 69.7, 69.8, 71.6, 73.0, 113.9, 114.2, 115.4, 121.3, 121.6, 128.9, 136.5, 148.7, 148.8; HRFAB:  $[\text{C}_{30}\text{H}_{42}\text{O}_9\text{Na}]^+ = 546.2801$ , calcd = 546.2829.

### **Analysis of Complexes between Ammonium Centers and Crown-Ether Monomers:**

**Representative Analysis of Complex Formation by ESI-MS:** A solution of **b-Am<sub>P11</sub>** with 2 equivalents of **DB24C8-CP** in 1:20  $\text{CHCl}_3$ :TFE was allowed to evaporated slowly under a stream of argon. The dry material was taken up in 3:1 MeOH: $\text{CH}_3\text{CN}$ . To make the injection sample, 1  $\mu\text{L}$  of the solution was diluted with 200  $\mu\text{L}$  of 4:1 MeOH: $\text{CH}_3\text{CN}$ . The sample was injected via syringe pump at 5  $\mu\text{L}/\text{min}$ . To facilitate complex formation, the following recommended settings for the spectrometer were used: capillary temperature (200° C) and tube lens offset (-39 V).<sup>14</sup> Because of limitations of the instrument, the ideal spray voltage setting of 0.01 kV could not be used; instead the default setting of 4.5 kV was used.

**Typical Procedure for Metathesis Experiments:** A solution containing the **DB24C8-derivative** (1.0 mmol) and template (0.5 mmol for bis-templates, 0.33 mmol for tris-templates) in DCM was stirred at ambient temperature for 0.5 h. The catalyst, dissolved in DCM, was added to the reaction mixture such that the final concentration of the crown derivative was 1.0 mM (or 0.5 mM for **DB24C8-diene**). The solution was heated to 40 °C for 2 h, before quenching the catalyst with ethyl vinyl ether (0.1 mL). The solvent was removed and the sample was subjected to HPLC analysis.

## V. References:

1. Cantrill, S. J.; Pease, A. R.; Stoddart, J. F., *J. Chem. Soc., Dalton Trans.*, **2000**, 3715-3734.
2. Ashton, P. R.; Chrystal, E. J. T.; Glink, P. T.; Menzer, S.; Schiavo, C.; Spencer, N.; Stoddart, J. F.; Tasker, P. A.; White, A. J. P.; Williams, D. J., *Chem. Eur. J.*, **1996**, *2*, 709-728.
3. Gutmann, V. W., E., *Inorg. Nuc. Chem. Lett.*, **1966**, *2*, 257-260.
4. Karle, I. L.; Flippenanderson, J. L.; Uma, K.; Balaram, P., *Biopolymers*, **1993**, *33*, 827-837.
5. Blackwell, H. E.; Sadowsky, J. D.; Howard, R. J.; Sampson, J. N.; Chao, J. A.; Steinmetz, W. E.; O'Leary, D. J.; Grubbs, R. H., *J. Org. Chem.*, **2001**, *66*, 5291-5302.
6. Brookhart, M.; Grant, B.; Volpe, A. F., *Organometallics*, **1992**, *11*, 3920-3922.
7. Cantrill, S. J.; Grubbs, R. H.; Lanari, D.; Leung, K. C. F.; Nelson, A.; Poulin-Kerstien, K. G.; Smidt, S. P.; Stoddart, J. F.; Tirrell, D. A., *Org. Lett.*, **2005**, *7*, 4213-4216.
8. Raymo, F. M.; Houk, K. N.; Stoddart, J. F., *J. Am. Chem. Soc.*, **1998**, *120*, 9318-9322.
9. Beil, J. B.; Lemcoff, N. G.; Zimmerman, S. C., *J. Am. Chem. Soc.*, **2004**, *126*, 13576-13577.
10. Toniolo, C.; Benedetti, E., *Trends Bioc. Sci.*, **1991**, *16*, 350-353.
11. Marqusee, S.; Robbins, V. H.; Baldwin, R. L., *Proc. Nat. Acad. Sci. U.S.A.*, **1989**, *86*, 5286-5290.
12. Wagner, G., *Prog. Nucl. Magn. Reson. Spectrosc.*, **1990**, *22*, 101-139.
13. Dalley, N. K.; Bradshaw, J. S.; Larson, S. B.; Simonsen, S. H., *Acta Crystallogr., Sect. B: Struct. Sci.*, **1982**, *38*, 1859-1862.
14. Julian, R. R.; Beauchamp, J. L., *Int. J. Mass Spectrom.*, **2001**, *210*, 613-623.
15. Badjic, J. D.; Nelson, A.; Cantrill, S. J.; Turnbull, W. B.; Stoddart, J. F., *Acc. Chem. Res.*, **2005**, *38*, 723-732.
16. Mulder, A.; Huskens, J.; Reinhoudt, D. N., *Org. Biomol. Chem.*, **2004**, *2*, 3409-3424.
17. Ercolani, G., *J. Am. Chem. Soc.*, **2003**, *125*, 16097-16103.
18. Grubbs, R. H., Ed., *Handbook of Metathesis*. Wiley-VCH: Weinheim, 2003.
19. Hong, S. H.; Sanders, D.P.; Lee, C.W.; Grubbs, R.H., *J. Am. Chem. Soc.*, **2005**, *127*, 17160 - 17161.
20. Saxena, I.; Borah, R.; Sarma, J. C., *Indian J. Chem., Sect. B*, **2002**, *41*, 1970-1971.

**Chapter 3**  
*A Boronate Ester Recognition Motif*

## **I. Introduction**

### **Alternate Recognition Motifs:**

Previous investigation of template-directed metathesis demonstrated the pseudorotaxane was a useful recognition motif for metathesis dimerization, but not for trimerization or longer polymerizations. The tris-templated reactions afforded high yields of a cyclic dimer product, and only small amounts of trimer. It was hypothesized that after the initial dimerization reaction, one of the crown-ether moieties was de-threading from one of the ammonium binding sites which allowed an intramolecular metathesis cyclization reaction to occur yielding a cyclic dimer. To eliminate the formation of cyclic dimer and therefore allow a higher yield of trimer, a more stable recognition motif was sought.

Experiments with palladium and platinum pincer binding motifs indicated that the pincer metal caused olefin isomerization, leading to the formation of myriad dimer products (Nelson, A., Hou, C., Grubbs, R.H, unpublished). For this reason, the pincer recognition motif was untenable for the metathesis template system. A cytosine-guanine recognition motif was also explored (Schmidt, S., Leung, K., Grubbs, R.H., Stoddart, J.F., unpublished). However, the limited solubility in aprotic solvents of the guanine half of the recognition unit made this motif unsuitable for metathesis polymerization.

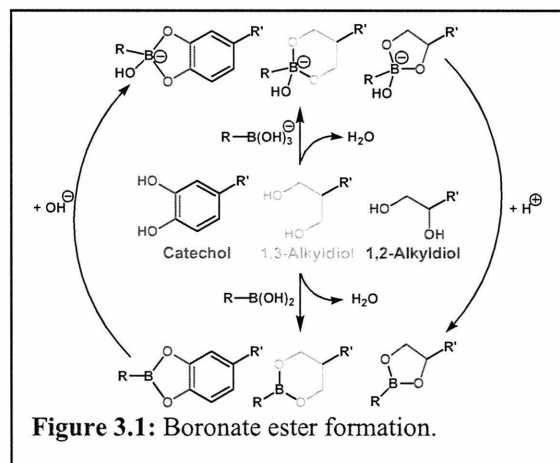
### **The Boronate Ester Recognition Motif:**

As an alternative, a boronate ester motif was examined. This interaction arises from a covalent reaction between a boronic acid and a diol and was anticipated to provide a stronger interaction than the pseudorotaxane, which is a non-covalent association. The pseudorotaxane needs low Gutmann donor number solvents to form a strong complex and

has an equilibrium that is shifted to favor the uncomplexed form in water. On the other hand, the boronate ester is covalently bound in anhydrous solvents and can also be formed in water (**Table 3.1**). The equilibrium in water is affected by the arrangement of the diol alcohols, with the catechol molecule forming the strongest boronate ester in water, followed by 1,2-diols and then 1,3-diols.<sup>1</sup>

Diol	$K_{eq}$ (M <sup>-1</sup> )
Catechol	830
D-sorbitol	370
D-fructose	160

**Table 3.1:** Equilibrium constants with phenylboronic acid in aqueous buffer, pH 7.4.



The boronate ester can be charged and in a tetrahedral geometry or can be neutral and in a trigonal planar geometry (**Fig. 3.1**). Within aprotic, organic solvents suitable for metathesis, the neutral boronate ester will have more favorable solubility properties. 1,2-diols favor the formation of charged, tetrahedral boronate esters while 1,3-diols favor formation of neutral, trigonal planar boronate esters.<sup>2,3</sup> Therefore, even though 1,2-diols form stronger boronate esters, the 1,3-diol functionality is more desirable for the template system.

An additional benefit of the boronate ester motif is that it does not involve additional metals and so avoids the complications seen with the pincer motif.

### Template Design:

To adapt the boronate ester functionality into the two component template and binding monomer system, the two functionalities – boronic acid and the diol – must be incorporated into the two components – a peptide template and an olefin monomer. Because the boronate ester strength can be tuned by changing the diol reagent and it was more synthetically accessible to make functionality changes to the olefin-containing monomer rather than the peptide template, the system was established to involve diol-olefin monomers and boronic acid containing peptides. An additional benefit to this configuration was that the commercially available L-(4-Boronophenyl)alanine reagent could be used to incorporate the boronic acid functionality into the templates.

The basic sequence of the series of peptide templates bearing boronic acid functionality (**Table 3.2**) was based upon the successful pseudorotaxane template, **b-Am<sub>P3</sub>**.

Type of Peptide	Chemical Formula	ID
3-mer	Ac-F( <i>p</i> BA)-A-F( <i>p</i> BA)-NH <sub>2</sub>	<b>b-BA<sub>P3</sub></b>
On-resin, 3-mer	Ac-F( <i>p</i> BA)-A-F( <i>p</i> BA)-Rink Amide MBHA	<b>MBHA-b-BA<sub>P3</sub></b>
On-resin, 5-mer	Ac-F( <i>p</i> BA)-A-F( <i>p</i> BA)-A-F( <i>p</i> BA)- Rink Amide MBHA	<b>MBHA-t-BA<sub>P5</sub></b>
On-resin, 5-mer	Ac-F( <i>p</i> BA)-A-F( <i>p</i> BA)-A-F( <i>p</i> BA)-Tenta	<b>Tenta-t-BA<sub>P5</sub></b>

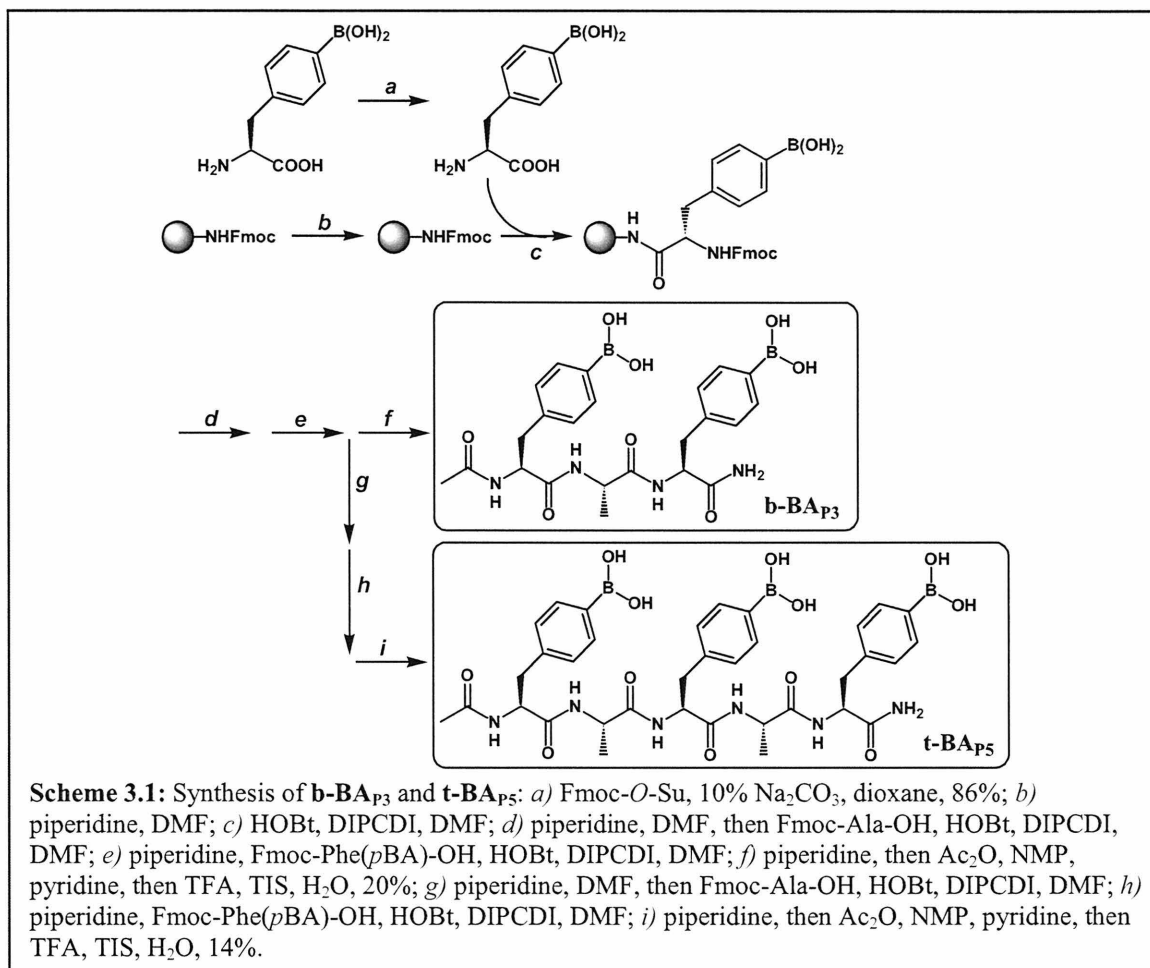
**Table 3.2:** The series of templates studied bearing boronic acid functionalities for boronate ester formation.

## II. Results and Discussion

### Template synthesis:

As a first step towards the synthesis of the peptides **BA<sub>P3</sub>** and **BA<sub>P5</sub>**, the free amine of L-(4-Boronophenyl)alanine was Fmoc-protected (**Scheme 3.1 a**). Using standard Fmoc solid phase synthesis on a Rink Amide MBHA resin, a tripeptide and

pentapeptide were synthesized (**Scheme 3.1 b-i**). After protecting the N-terminus with an acetyl group, acidic conditions were used to cleave the peptide from the resin with a C-terminal amide. Reverse phase HPLC purification yielded the desired peptides.



### On-resin Template Synthesis:

Using a resin-bound template is an effective method to drive up the yield of a reaction and to avoid unwanted side-product contaminants.<sup>4-6</sup> In this approach, any non-associated monomers and their template-independent products may be washed away at the end of the reaction so that they do not contaminate the templated-dependent product profile. Controlled removal of the bound daughter polymer yields a completely template-directed product.

To generate a useful on-resin peptide template, the same procedure as before was followed for the amino acid couplings to synthesize the **b-BA<sub>P3</sub>** and **t-BA<sub>P5</sub>** peptides on Rink Amide MBHA resin. However, the original peptide synthesis used pyridine in the final N-terminal acetyl protection step. It was found that in order to perform metathesis on-resin, pyridine had to be excluded from the peptide synthesis because having the amine base trapped within the resin poisoned the catalyst.<sup>7</sup> To avoid the use of pyridine, the synthesis was revised to use a pentafluorophenyl acetate reagent<sup>8,9</sup> to acetylate the N-terminus instead of acetic anhydride in pyridine.

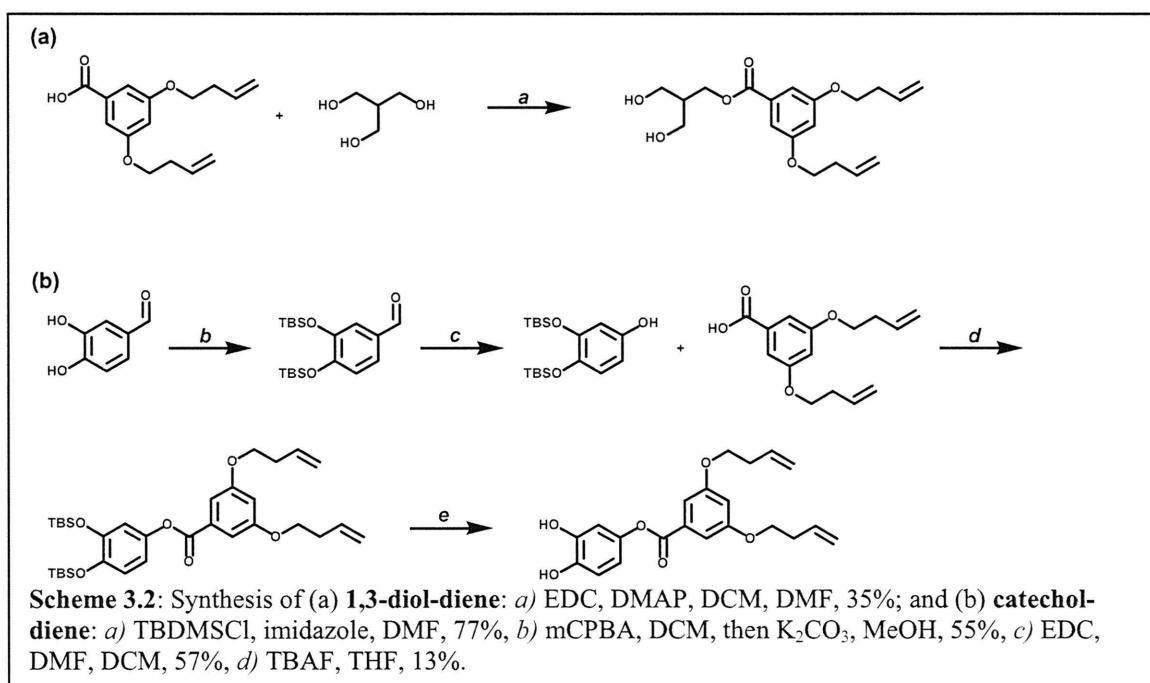
A second type of resin, TentaGel S RAM, was also used as a template-presentation platform. The TentaGel S resin is composed of a lightly crosslinked polystyrene matrix with alkyl-linked PEG grafts. The resin contains ~50-70% PEG and its properties are highly influenced by the PEG moieties. These properties manifest themselves in swelling behavior that is almost independent of the solvent used to swell the matrix and in the solution-like reactivity of the reactive sites. The **b-BA<sub>P3</sub>** peptide was synthesized on the TentaGel S resin using the same procedure established on the Rink Amide BMHA resin.

### **Monomer syntheses:**

An ADMET monomer containing a diol functionality (**1,3-diol-diene**) was synthesized (**Scheme 3.2a**) Starting from the 1-bromobutene alkylated 3,4-dihydroxybenzoic acid compound used in the synthesis of **DB24C8-diene**, a symmetrical ADMET-diol monomer was synthesized in one step via esterification with 2-hydroxymethyl-1,3-propanediol. Having a symmetrical diol-monomer simplified the

analysis of the boronate ester and the subsequent metathesis products; use of an unsymmetrical diol would yield diastereomeric boronate esters and metathesis products.

A second monomer (**catechol-diene**) was also synthesized, using a catechol in place of the 1,3-diol (**Scheme 3.2b**) It was anticipated that using this diol functionality would give more stable boronate esters. To synthesize the compound, the alcohol groups of 3,4-dihydroxybenzaldehyde were silyl protected and the aldehyde was reduced to an alcohol. The resulting compound was coupled to the ADMET-acid intermediate and the silyl groups were removed to yield the desired product. **Catechol-diene** turned out to be unstable and difficult to store, and so was not used in the metathesis studies.



### Boronate Ester Formation in Solution:

Commercially available 7-octene-1,2-diol was used to establish the optimal conditions to form the boronate ester in solution.  $^1H$  NMR confirmed complete boronate

ester formation after the **b-BA<sub>P3</sub>** peptide and **1,3-diol-diene** were heated at 40 °C for two hours with molecular sieves in a solution of dichloromethane and methanol.

#### **Boronate Ester Formation On-Resin:**

Optimal on-resin boronate ester formation and hydrolysis conditions were studied using the **MBHA-b-BA<sub>P3</sub>** template via HPLC analysis. In a series of steps, a standard metathesis reaction was replicated: **1,3-diol-diene** was complexed to **MBHA-b-BA<sub>P3</sub>**, the monomer solution was collected and the resin was washed, the on-resin boronate ester complex was subjected to mock metathesis conditions (40 °C in DCM for 2hr, no catalyst), and the boronate ester was hydrolyzed to elute all diol-containing molecules.

Using this method the ideal conditions for forming the boronate ester on-resin were found to be mixing for 4 hours at 40 °C in dichloromethane with 4 Å molecular sieves and the ideal reagent to hydrolyze the boronate ester complex was found to be a 60% acetonitrile solution in aqueous 1% TFA. The HPLC trace of the elution solution showed a strong peak for **1,3-diol-diene**, integration of which indicated that 95% of the monomer loaded onto the resin was recovered (**Fig. 3.2**). In addition, only a small amount of **1,3-diol-diene** was seen in the mock metathesis solution, indicating that the boronate ester is stable under those conditions.

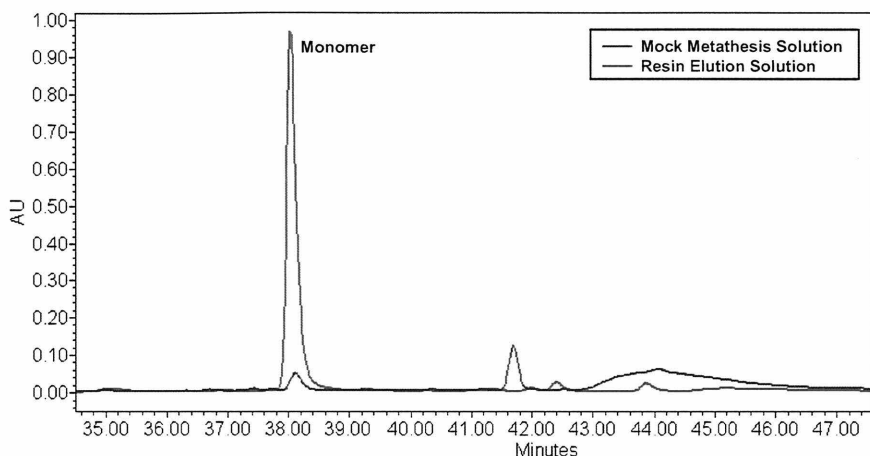


**Figure 3.2:** HPLC analysis of on-resin mock metathesis reaction and diol elution of **1,3-diol-diene** and **MBHA-b-BP3**.

In an experiment with unmodified MBHA Rink Amide resin, neither the mock metathesis solution nor the elution solution showed any **1,3-diol-diene** monomer by HPLC analysis. This demonstrated that the **1,3-diol-diene** monomer bound selectively to the peptide attached to the resin, and was not interacting non-selectively with the resin.

#### **Template-Directed Cross Metathesis:**

To test the ability of the boronate ester system to directed metathesis dimerization, the boronate ester complex formed from 7-octene-1,2-diol and **b-BA<sub>P3</sub>** was subjected to cross metathesis conditions with 25 mol % catalyst **3**. The reaction was run with an olefin concentration of 1 mM, and the reaction was analyzed by <sup>1</sup>H NMR.

Because the reaction was dilute, it had to be quenched and concentrated before analysis.

<b>b-BA<sub>P3</sub></b>	Yield (%) Dimer
–	25
+	65

**Table 3.3:** Influence of boronate ester template on cross metathesis. Reactions were run with 1mM 7-octene-1,2-diol and 25 mol % **3** at 40 °C.

This experiment demonstrated the applicability of the boronate ester motif to the template-directing system. Complexation of 7-octene-1,2-diol to **b-BA<sub>P3</sub>** prior to the metathesis reaction increased the yield of dimer by more than 2.5 times (**Table 3.3**).

#### **Template-Directed ADMET:**

ADMET dimerization reactions were run with **b-BA<sub>P3</sub>** and **1,3-diol-diene** and analyzed by HPLC. The results from the templated reactions were not as selective as those seen in the cross metathesis reactions. Specifically, the dimerization yields were consistently as high without template as with. This was unexpected given the high association constant of boronate esters.

However, the template did influence the distribution of products. The reaction without template yielded exclusively a cyclic dimer, while the reaction with **b-BA<sub>P3</sub>** yielded a mixture of linear and cyclic dimers (**Table 3.4**). Attempts to increase the yield in the reaction with template – longer reaction time and using different metathesis catalysts – were not successful.

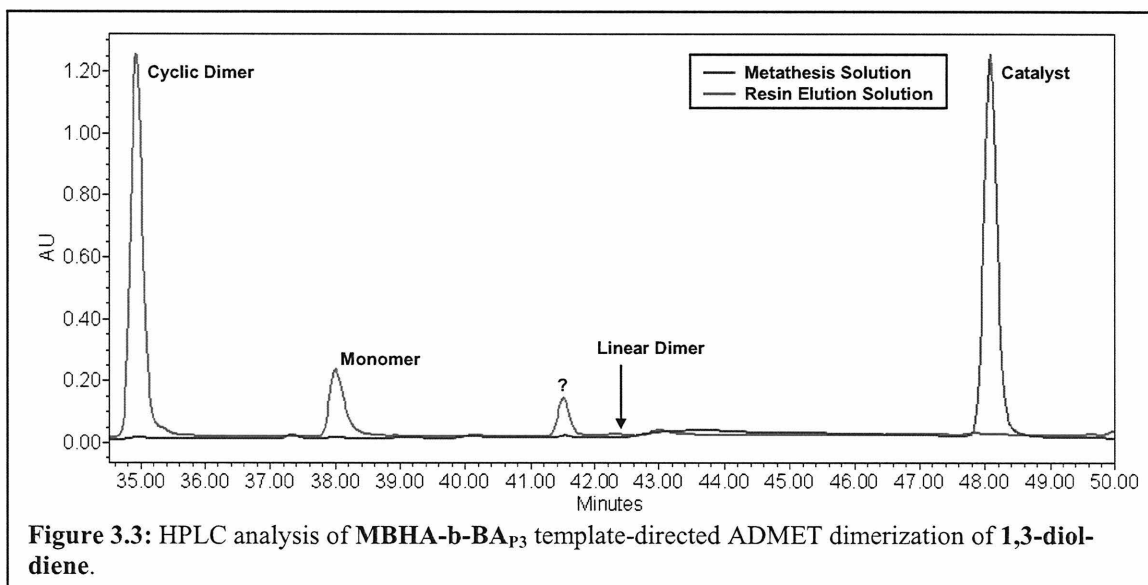
<b>b-BA<sub>P3</sub></b>	Yield (%) Linear Dimer	Yield (%) Cyclic Dimer	Overall Yield (%)
–	0	56	56
+	15	22	37

**Table 3.4:** Influence of peptide template of ADMET dimerization of 1mM **1,3-diol-diene**.

The possibility was investigated that the high background reaction was due to an association between the diol functionality of the free monomer and the catalyst. In a reaction without template, *p*-phenylboronic acid (PBA) was complexed to the monomer prior to the metathesis reaction to block the interaction. However, addition of PBA had no effect on the background reaction.

### On-Resin Template-Directed ADMET:

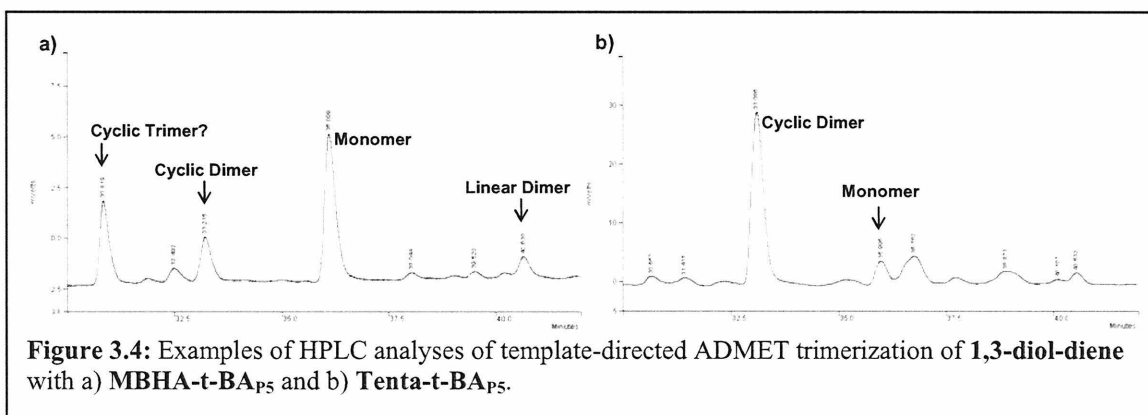
Using the conditions previously established, a boronate ester complex was formed between **MBHA-b-BA<sub>P3</sub>** and **1,3-diol-diene**. Analysis of the elution solution from the on-resin ADMET dimerization with this complex showed an 83% yield of cyclic dimer (**Fig. 3.3**). In addition, the solution from the metathesis step of the reaction (i.e., before boronate ester hydrolysis) showed a large catalyst peak, but no peaks from diol-containing compounds. Interestingly, unlike the template-directed reactions in solution, the reaction on solid support yielded only cyclic dimer. The yield was significantly higher than that seen for the reactions in solution. The reaction on-resin also appeared to be much cleaner – with fewer side products – than those in solution.



The effective template-directed metathesis dimerization using on-resin bis-templates did not transfer to the tris-templates, **MBHA-t-BA<sub>P5</sub>** and **Tenta-t-BA<sub>P5</sub>**. In general, the recovery of the diol-containing compounds was impaired compared to that with the bis-templates was lower and trimer products could be identified.

Across trials, the reactions with **MBHA-t-BA<sub>P5</sub>** were reproducible, giving a similar HPLC profiles each time. In those reactions there was always a significant amount of **1,3-diol-diene** monomer and a new large peak at eluted after 30 minutes (**Fig. 3.4a**). While this seemed like an appropriate retention time for a cyclic trimer product, the identity of this peak could not be confirmed by MS.

The reactions with **Tenta-t-BA<sub>P5</sub>** were more variable. In some reactions a significant amount of **1,3-diol-diene** monomer remained and in others a high yield of cyclic dimer was seen (**Fig. 3.4b**). However, no new peak of significant size was seen in any of the reactions with **Tenta-t-BA<sub>P5</sub>**.



### III. Conclusions

As with the pseudorotaxane recognition motif, the boronate ester motif showed a significant template effect for metathesis dimerization, but not for trimerization. Efforts to reduce the level of background and side reactions by using a resin-attached template improved the dimerization reactions with a bis-template but did not yield trimers when used with tris-templates.

## IV. Experimental

**Fmoc-L-(4-Boronophenyl)alanine:** A solution of Fmoc N-hydroxysuccinimide ester (334.1 mg, 0.99 mmol) in 3.0 mL dioxane was added to a solution of L-(4-Boronophenyl)alanine (207.0 mg, 0.99 mmol) in 1.9 mL 10% Na<sub>2</sub>CO<sub>3</sub> (aq) solution. The reaction was stirred overnight. It was then diluted with water and washed with diethyl ether (3x). The pH of the aqueous layer was adjusted to 3 with 1M HCl, which caused a white precipitate to form. The precipitate was removed by filtration, dissolved in EtOAc, dried over Na<sub>2</sub>SO<sub>4</sub> and concentrated to a translucent film. The material was dissolved in MeOH/EtOAc, and the insoluble white crystals were removed by filtration. Concentration of the solution yielded 368.3 mg of product as a white solid (86%): <sup>1</sup>H NMR (CD<sub>3</sub>OD) δ 7.77 (4H, d), 7.57 (2H, d), 7.23-7.43 (6H, m), 4.45 (1H, dd, *J* = 4.8, 9.9 Hz), 4.28 (1H, dd), 4.10-4.4.23 (3H, m), 3.23 (1H, dd, *J* = 4.8, 14.1 Hz), 2.94 (1H, dd, *J* = 9.9, 13.8 Hz).

**Peptide Syntheses:** The peptides for **b-BA<sub>P3</sub>** and **t-BA<sub>P5</sub>** were synthesized using standard Fmoc-solid phase synthesis techniques. After cleavage, the peptide was precipitated from the crude orange oil with chilled ether and then was further purified by RP HPLC.

**b-BA<sub>P3</sub>:** The reaction yielded 16.0 mg (0.0312 mmol) of peptide as a white powder (20%).

**t-BA<sub>P5</sub>:** The reaction yielded 11.0 mg of peptide as an off-white powder (17%).

**Pentafluorophenyl acetate:** A solution of pentafluorophenol and acetic anhydride (0.5 eq.) in CH<sub>3</sub>CN was added to a solution of DCC (0.5 eq.) in CH<sub>3</sub>CN under anhydrous conditions. After stirring for 2 hours at rt, the product was isolated by silica gel column chromatography to yield 121 mg of a white solid (67%).

**1,3-diol-diene:** The ADMET-acid compound (0.0782 mmol) was dissolved in anhydrous DCM. EDC (2.0 eq.) and DMAP (0.1 eq.) were added to the solution. After stirring for 10 minutes, a solution of 2-hydroxymethyl-1,3-propanediol (2.0 eq.) in DMF was added. After stirring for 3 hours at r.t., the product was isolated by column chromatography in 1:1 EtOAc:Hex (35%).

## V. References

1. Springsteen, G., Wang, B., *Tetrahedron*, **2002**, *58*, 5291-5300.
2. Dale, J., *J. Chem. Soc.*, **1961**, 922-&.
3. Bachelier, N.; Verchere, J. F., *Polyhedron*, **1995**, *14*, 2009-2017.
4. Yang, W. Q.; Gao, X. M.; Springsteen, G.; Wang, B. H., *Tetrahedron Lett.*, **2002**, *43*, 6339-6342.
5. Gravel, M.; Thompson, K. A.; Zak, M.; Berube, C.; Hall, D. G., *J. Org. Chem.*, **2002**, *67*, 3-15.
6. Carboni, B.; Pourbaix, C.; Carreaux, F.; Deleuze, H.; Maillard, B., *Tetrahedron Lett.*, **1999**, *40*, 7979-7983.
7. Armstrong, S. K., *J. Chem. Soc., Perkin Trans. 1*, **1998**, 371-388.
8. Shelkov, R.; Nahmany, M.; Melman, A., *Org. Biomol. Chem.*, **2004**, *2*, 397-401.
9. Kisfaludy, L.; Mohacsi, T.; Low, M.; Drexler, F., *J. Org. Chem.*, **1979**, *44*, 654-656.